Pinning of flux lines by planar defects

Aleksandra Petković,[1] Thorsten Emig,[1,2] and Thomas Nattermann[1]

[1]*Institut für Theoretische Physik, Universität zu Köln, Zülpicher Straße 77, 50937 Köln, Germany*

[2]*Laboratoire de Physique Théorique et Modèles Statistiques, CNRS UMR 8626, Université Paris-Sud, 91405 Orsay, France*

The influence of randomly distributed point impurities and planar defects on order and transport in type-II superconductors and related systems is studied. It is shown that the Bragg glass phase is unstable with respect to planar defects. Even a single weak defect plane oriented parallel to the magnetic field as well as to one of the main axes of the Abrikosov flux-line lattice is a relevant perturbation in the Bragg glass. A defect that is aligned with the magnetic field restores the flux density oscillations, which decay algebraically with the distance from the defect. The theory exhibits striking similarities to the physics of a Luttinger liquid with a frozen impurity. The exponent for the flux-line creep in the direction perpendicular to a relevant defect is derived. We find that the flux-line lattice exhibits in the presence of many randomly distributed parallel planar defects aligned to the magnetic field a glassy phase which we call *planar glass*. The planar glass is characterized by diverging shear and tilt moduli, a transverse Meissner effect, and resistance against shear deformations. We also obtain sample-to-sample fluctuations of the longitudinal magnetic susceptibility and an exponential decay of translational long-range order in the direction perpendicular to the defects. The flux creep perpendicular to the defects leads to a nonlinear resistivity $\rho(J \to 0) \sim \exp[-(J_D/J)^{3/2}]$. Strong planar defects enforce arrays of dislocations that are located at the defects with a Burgers vector parallel to the defects in order to relax shear strain.

I. INTRODUCTION

Type-I superconductors are both perfect conductors and perfect diamagnets. In type-II superconductors the perfect diamagnetism is reduced, an external magnetic field penetrates the sample above the lower critical field H_{c1} in the form of magnetic-flux lines (FLs).[1] A transport current will then lead to a motion of the FLs, yielding a linear resistivity $\rho \approx \rho_n B/H_{c2}$ in disorder-free samples. Here B denotes the magnetic induction and H_{c2} is the upper critical field.[2] At $B = H_{c2}$ diamagnetism disappears completely and ρ reaches the resistivity ρ_n of the normal state. In order to recover the desired property of a dissipation-free flow, FLs have to be pinned. Point defects, such as vacancies or interstitials, are one type of pinning source. In high-T_c materials point impurities are almost always present due to a nonstoichiometric composition of most materials. Impurity pinning leads to a zero linear resistivity.[3] However, thermal fluctuations allow for FL creep, resulting in a nonzero *nonlinear* resistivity of the form $\rho(J) \sim \exp[-(J_P/J)^\mu]$, where the creep exponent is $\mu = 1/2$ for point impurities.[4] $J(\ll J_P)$ denotes the current density and J_P depends on B, temperature T, concentration and strength of the pinning centers, as well as on properties of the material through the superconductor coherence length ξ and the penetration length λ. This FL creep law is closely related to the order of the flux-line lattice (FLL) in the presence of point pinning centers.

The order of the FLL was a puzzle for a long time. Larkin concluded in 1970 that randomly distributed impurities destroy the long-range order of the Abrikosov lattice.[5] Only much later it was realized that the effect of impurities is weaker, resulting in a power-law decay of translational order of the FLs in the so-called "Bragg glass" phase.[4,6–10]

More effective pinning sources can further suppress the nonlinear resistivity. One example are columnar defects, pro-duced by heavy-ion radiation, that have been considered by Nelson and Vinokur.[11,12] These authors mapped the physics of FLs onto the problem of the localization of bosons in two dimensions where FLs play the role of world lines of the bosons. A similar approach was proposed also by Lyuksyutov (Ref. 13). At low temperatures they found strongly localized FLs at the columnar defects, forming a "Bose glass" phase.[11,12] Thermally activated hopping of noninteracting FLs in the limit $J \to 0$ leads to the creep exponent $\mu = 1/3$, while FL interactions yield the increased creep exponent $\mu = 1$.[3] The transport in this regime closely resembles the variable range hopping of electrons in two-dimensional disordered semiconductors. This picture is expected to be valid for weak enough applied magnetic fields, such that the density of defects is bigger than the FL density. For a larger magnetic field, Radzihovsky[14] argued that the Bose glass coexists with a resistive liquid of interstitial FLs which upon cooling freezes into a weakly pinned Bose glass. For asymptotically weak currents, the creep of FL bundles determines the nonlinear resistivity and $\mu = 1$ is the creep exponent.[3]

In this work we consider planar defects such as twin boundaries from which even stronger pinning can be expected. Twin boundaries are ubiquitous in superconducting $YBa_2Cu_3O_{7-x}$ and La_2CuO_4, where they are needed to accommodate strains arising from tetragonal to orthorhombic transition as a result of oxygen vacancy ordering and due to rotation of the CuO_6 octahedra, respectively.[15] Twin boundaries occur frequently with the same orientation[16–18] or in orthogonal families of lamellas ("colonies").[15,19] They can be regularly distributed with rather fixed spacing or with large variations in the spacing.[20] The mean distance ℓ_D of the defect planes varies between 10 nm[16,17,19] and 1 μm.[18,21]

The common feature of all of the above mentioned defects is that they lead to FL pinning, but what distinguishes them is the nature of the pinned phase. In contrast to point

disorder, which promotes FL wandering, planar defects inhibit wandering and promote localization. Pinning of individual FLs by columnar as well as planar defects in the presence of bulk point disorder has been investigated in the past.[22–25] The competition between a planar defect and point impurities in three-dimensional systems, for a single FL, leads to localization of the FL at all temperatures.[22–24] The influence of many parallel defect planes on the creep of a single FL perpendicular to the planes has been studied at low temperatures when the FL spacing exceeds the average spacing between the planes.[20]

The main focus of this paper is correlated disorder in the form of planar defects. Some of the results of this paper have been published earlier.[26,27] Here we give additional results and present more detailed derivations. First, we discuss the influence of a single planar defect on the stability of the Bragg glass (BG) phase. Then we explore the effect of many defect planes on the FLL. We find that the necessary condition for a weak planar defect to become a relevant perturbation is that it is oriented parallel to the magnetic field. In this case, its influence on the Bragg glass phase can be characterized by the value of a single parameter $g \equiv \frac{3}{8}\eta(a/\ell)^2$, which depends both on the exponent η describing the decay of the positional correlations in the Bragg glass phase and on the orientation of the defect with respect to the FLL. a and ℓ are the mean spacing of the FLs in the absence of the defect plane and the distance between lattice planes, of the Abrikosov lattice, parallel to the defect, respectively. A weak defect turns out to be relevant if $g < 1$, i.e., if it is parallel to one of the main crystallographic planes of the FLL.

The FL density averaged over point impurities shows periodic order with an amplitude decaying as a power law with the normal distance to the defect plane. For a relevant defect on scales larger than L_v, the exponent controlling the power law is g. For the definition of L_v, see Eq. (38) below. For $g > 1$ a weak defect is irrelevant (in the sense of renormalization group) and the density profile decays faster, with a larger exponent $2g - 1 > 1$, on scales larger than the positional correlation length L_a. For a weak defect tilted against the applied magnetic field we find that FL density oscillations decay exponentially fast. We investigate also the dynamics of FL bundles perpendicular to the relevant defect for small current densities $J \to 0$. The nonlinear resistivity is $\rho(J) \sim \exp[-\frac{C_1}{J}(\log\frac{C_2}{J})^2]$, where C_1 and C_2 depend on various parameters such as temperature, magnetic induction, density and strength of point impurities, as well as the strength of the defect plane. We conclude that a single relevant defect plane slows down the FL creep in comparison to the BG phase.

There are interesting connections of some of the aspects of our results to related two-dimensional classical or one-dimensional quantum models. A single planar defect in the Bragg glass phase resembles the presence of a single columnar defect in a FLL confined to a plane[28–30] or a frozen impurity in a Luttinger liquid.[31,32] In all three cases the bulk phases on both sides of the defect are characterized by logarithmically diverging displacement correlations. The parameter g plays the role of a temperature in the two-dimensional (2D) classical case and of the Luttinger liquid parameter in the one-dimensional (1D) quantum case. The periodic order
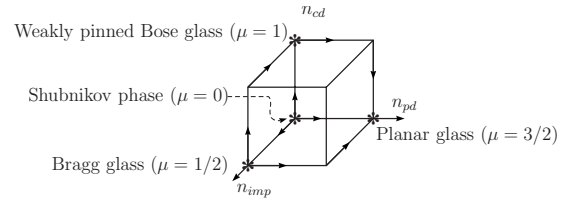

FIG. 1. Schematic phase diagram of disordered flux-line lattices resulting from impurities, columnar and planar defects of concentration n_{imp}, n_{cd}, and n_{pd}, respectively. The stability of the phases with respect to different kinds of disorder is indicated by arrows. μ denotes the creep exponent.

seen around the defect plane has its counterpart in Friedel oscillations around an impurity in Luttinger liquids. Whereas in the 1D (2D) case the relevance of an impurity is controlled by tuning the interaction strength (temperature), in the present case a change in g can be accomplished by changing the orientation of the defect with respect to the FLL. Transport properties of our system are however different from the ones in the related systems.

In this article we also study the effect of a finite density of randomly distributed parallel planar defects on the FLL at low temperatures with the magnetic field aligned parallel to the defects. We consider the case when the mean defect spacing is much greater than FL spacing. Our results may be directly applicable to a wide class of other systems with planar defects as a stack of membranes under tension, charge-density waves,[33] and domain walls in magnets and incommensurate systems[34] since we consider a simplified model with a uniaxial displacement field perpendicular to the defects. We find a phase, which we call *planar glass*, that is characterized by (i) diverging shear (tilt) modulus that determines the energy cost for a shearing (tilting) of the FLL in the direction perpendicular to the planes; (ii) finite compressibility; (iii) sample-to-sample fluctuations of the longitudinal magnetic susceptibility; (iv) an exponential decay of positional correlations in the direction perpendicular to the defects; and (v) a creep exponent $\mu = 3/2$ for creep in the direction perpendicular to the defects for small currents $J \to 0$. The planar glass is different from the Bragg glass or the Bose glass phase and from the phase found for equally spaced defects.[35] The planar glass is stable over a finite range of tipping angles of the applied magnetic field away from the direction parallel to the planar defects, i.e., it is characterized by a transverse Meissner effect. Similarly, the planar glass is characterized by a resistance against shear deformations that are perpendicular to the defects. Naturally, realistic samples contain both point and correlated disorder (as columnar and/or planar defects). We find that the planar glass is stable against both weak point and weak columnar disorder. The schematic phase diagram is shown in Fig. 1. When we consider a *vector* displacement field, we additionally find that strong disorder enforces arrays of dislocations in order to relax shear strain. They are located at the defects with a Burgers vector parallel to the defects. We argue that the main properties of the planar glass remain unchanged by dislocations.

The paper is organized as follows. In Sec. II we introduce a model for interacting FLs that couple to weak point impu-

rities and briefly review known results of this model. In Sec. III we consider a single defect plane as a perturbation to the Bragg glass phase and study the FL order using the a renormalization-group analysis. A finite density of randomly distributed defects is explored in Sec. IV and the planar glass is characterized. Functional renormalization-group equations are derived in $d = 6 - \epsilon$ dimensions. The response to tilt and shear deformations is discussed as well as sample-to-sample fluctuations of the longitudinal magnetic susceptibility. The positional correlation functions are computed and the stability of planar glass with respect to point and columnar disorder is studied. In Sec. V we consider the limit of *strong* planar defect potentials. In Sec. VI we consider the FL dynamics for small currents by investigating FL creep in the presence of a single defect plane, both with and without point impurities, and in the presence of a finite density of planes. Finally, in Sec. VII we discuss a model with a vector displacement field. Technical details and list of recurrent symbols are relegated to Appendixes A and G.

II. BRAGG GLASS PHASE

In this section we summarize some known results on pinning effects due to randomly distributed point impurities for interacting FLs. We use elasticity theory to describe a dislocation free array of FLs (for a review see, e.g., Blatter *et al.*[3]). Undistorted FLs are exactly parallel to the z axis which we assume to be the direction of the applied magnetic field. The FLs form a triangular Abrikosov FLL in the xy plane with a lattice constant a. In order to describe distortions of the FLs from the perfect lattice positions $\mathbf{R}_\nu$, we use a two-component vector displacement field $\mathbf{u}_\nu(z)$. Since we are interested in the behavior on large length scales, it is appropriate to describe the interacting FLs in terms of a continuum elastic approximation with a continuous displacement field $\mathbf{u}_\nu(z) \rightarrow \mathbf{u}(\mathbf{r})$.

The Hamiltonian

$$\mathcal{H} = \mathcal{H}_0 + \mathcal{H}_P \qquad (1)$$

consists of the elastic energy of the FLL, $\mathcal{H}_0$, and pinning energy of point impurities, $\mathcal{H}_P$. The elastic energy of the dislocations free FLL reads

$$\mathcal{H}_0 = \frac{1}{2} \int \frac{d^2 \mathbf{q}_\perp dq_z}{(2\pi)^3} \tilde{\mathbf{u}}(\mathbf{q}) (\tilde{\mathcal{G}}_L^{-1} \mathbf{P}_L + \tilde{\mathcal{G}}_T^{-1} \mathbf{P}_T) \tilde{\mathbf{u}}(-\mathbf{q}), \qquad (2)$$

where $\mathbf{q}_\perp = q_x \hat{\mathbf{x}} + q_y \hat{\mathbf{y}}$. $\mathbf{P}_L^{ij} = q_i q_j / q_\perp^2$ and $\mathbf{P}_T^{ij} = \delta_{ij} - q_i q_j / q_\perp^2$ are projectors onto the longitudinal and transversal modes, respectively, with propagators

$$\tilde{\mathcal{G}}_L^{-1} = c_{11} \mathbf{q}_\perp^2 + c_{44} q_z^2, \qquad (3)$$

$$\tilde{\mathcal{G}}_T^{-1} = c_{66} \mathbf{q}_\perp^2 + c_{44} q_z^2. \qquad (4)$$

In general, the compression (c_{11}) and the tilt (c_{44}) moduli are nonlocal on length scales smaller than the penetration depth λ but the shear modulus c_{66} is local. However, the dispersion of c_{11} and c_{44} on small length scales is negligible for the present problem since we are interested in asymptotic

properties at large length scales and small currents. Hence, in the following we introduce a cutoff in momentum space given by $\Lambda \approx 2\pi / \lambda$ and neglect the nonlocality of the elastic moduli. The elastic Hamiltonian of Eq. (2) can be obtained from symmetry arguments.[36] The ideal FLL is isotropic in xy plane and has D_{6h} symmetry group.

The pinning energy of randomly distributed point impurities is modeled by the coupling

$$\mathcal{H}_P = \int d^3 \mathbf{r} \rho(\mathbf{r}, \mathbf{u}) V_P(\mathbf{r}) \qquad (5)$$

of the local FL density $\rho(\mathbf{r}, \mathbf{u}) = \sum_\nu \delta[\mathbf{x} - \mathbf{R}_\nu - \mathbf{u}_\nu(z)]$ to the pinning potential $V_P(\mathbf{r})$, where $\mathbf{x} = (x, y)$. From this definition and the Poisson summation formula,[7,8] the density can be also written as

$$\rho(\mathbf{r}, \mathbf{u}(\mathbf{r})) = \rho_0 + \rho_0 \left\{ -\nabla_\mathbf{x} \mathbf{u}(\mathbf{r}) + \sum_{\mathbf{G} \neq 0} e^{i\mathbf{G}[\mathbf{x} - \mathbf{u}(\mathbf{r})]} \right\}, \qquad (6)$$

where $\rho_0 = 2/(\sqrt{3} a^2)$ and $\mathbf{G}$ is a vector of the reciprocal lattice. $V_P = -v_p \sum_i \delta_\xi(\mathbf{x} - \mathbf{x}_i) \delta(z - z_i)$ represents the pining potential due to randomly distributed point impurities. The δ functions are considered to have a finite width of the order of the superconductor coherence length ξ. For simplicity we subtract the average of the random potential and look at fluctuations around the average value. The pinning potential then satisfies

$$\overline{V_P(\mathbf{r})} = 0, \quad \overline{V_P(\mathbf{r}) V_P(\mathbf{r}')} = n_{imp} v_p^2 \delta_\xi(\mathbf{x} - \mathbf{x}') \delta(z - z'). \qquad (7)$$

The strength of the disorder is characterized by $v_p^2 n_{imp}$. Higher-order correlations of the (unrenormalized) pinning potential are nonzero but for weak disorder they can be neglected. The restriction to two-point correlations of V_P leads to the same replica Hamiltonian one obtains when V_P would be Gaussian distributed.

The model given by Eqs. (1)–(7) has been studied in detail using perturbation theory,[5] Flory-type arguments,[4,37] a Gaussian variational ansatz,[6,7,38] and functional renormalization group.[6–9] The correlations of the FLL fluctuations change with length scale and are characterized by three different regimes: the Larkin or random force (RF) regime, the random manifold (RM) regime, and the BG phase. These regimes are distinguished by the scaling behavior of

$$\overline{\langle (\mathbf{u}(\mathbf{r}) - \mathbf{u}(0))^2 \rangle} \propto |\mathbf{r}|^{2\zeta}, \qquad (8)$$

which defines the roughness exponent ζ. Here $\langle \ldots \rangle$ denotes a thermal and $\overline{\cdots}$ denotes a disorder average.

(i) In the Larkin regime[5] the displacements are sufficiently small so that the FLs stay within one minimum of the disorder potential $V_P(\mathbf{r})$ and perturbation theory can be applied. The effect of the disorder potential on the FLL is properly described by a random force $\mathbf{F}_P(\mathbf{R}_\nu, z) = -\nabla_\mathbf{x} V_P(\mathbf{R}_\nu, z)$. The roughness exponent is $\zeta_{RF} = (4 - d)/2$, where d denotes dimension of the system, so that the positional correlation function

$$S_{\mathbf{G}}(\mathbf{r}) = \overline{\langle e^{i\mathbf{G}\mathbf{u}(\mathbf{r})} e^{-i\mathbf{G}\mathbf{u}(0)} \rangle} \tag{9}$$

decays exponentially fast in $d=3$. The Fourier transform of $S_{\mathbf{G}}(\mathbf{r})$ is the structure factor which can be directly measured in diffraction experiments. The Larkin lengths L_ξ^z and L_ξ^x are defined as the crossover length scales where the conditions $\overline{\langle [\mathbf{u}(0, z=L_\xi^z) - \mathbf{u}(0)]^2 \rangle} \propto \xi^2$ and $\overline{\langle [\mathbf{u}(|\mathbf{x}|=L_\xi^x, 0) - \mathbf{u}(0)]^2 \rangle} \propto \xi^2$ are satisfied. This leads to

$$L_\xi^z \simeq \frac{\phi_0 \xi^6}{B v_p^2 n_{imp}} \frac{c_{44} c_{66}}{1 + \kappa},$$

$$L_\xi^x \simeq \frac{\phi_0 \xi^6}{B v_p^2 n_{imp}} \frac{c_{44}^{1/2} c_{66}^{3/2}}{1 + \kappa^{3/2}}, \tag{10}$$

where $\phi_0 = hc/(2e) = 2.07 \ 10^{-7}$ G cm^2 is the flux quantum and $\kappa = c_{66}/c_{11}$. The length L_ξ increases with decreasing disorder strength. An increase in the magnetic induction B effectively increases the disorder strength so that L_ξ shrinks.

(ii) On scales greater than the Larkin length, a description in terms of random forces become inapplicable and the RM regime applies. In the RM regime FLs explore many minima of the disorder potential but the typical displacement is still smaller than the FL spacing a. Hence the FLs do not compete with neighboring FL for identical pinning centers. A Flory-type argument[39,40] yields the roughness exponent $\zeta_{RM} = (4-d)/6$ but in Ref. 8 it was shown within an $\epsilon = 4-d$ expansion that ζ_{RM} depends on the ratio $\kappa = c_{66}/c_{11}$ and varies between 0.1737ϵ and 0.1763ϵ. The positional order decays according to a stretched exponential,

$$S_{\mathbf{G}}(\mathbf{r}) \sim \exp\left[-\frac{G^2 r^{2\zeta_{RM}}}{2} \right]. \tag{11}$$

(iii) On length scales larger than the positional correlation length L_a the RM regime becomes inapplicable. $L_a^{z,\mathbf{x}} \approx L_\xi^{z,\mathbf{x}} (a/\xi)^{1/\zeta_{RM}}$ is defined as the scale at which the mean-square displacement of FLs is of the order a. Therefore, it is crucial to keep the periodicity $\mathbf{u} \to \mathbf{u} + \mathbf{R}_\nu$ of the interaction between FLs and point disorder.[4] This leads to a much slower *logarithmic* increase ($\zeta_{BG} = 0$) of the elastic displacement of the FLs than in the Larkin and RM regime. It was shown[4,6–9,38] that thermal fluctuations are irrelevant and that the pinned FLL exhibits a power-law decay of positional correlations,

$$S_{\mathbf{G}}(\mathbf{x}, 0) \sim |\mathbf{x}|^{-\eta_{\mathbf{G}}}, \tag{12}$$

where $\eta_{\mathbf{G}} = \eta (G/G_0)^2$ and $G_0 = 4\pi/(\sqrt{3}a)$. This result resembles the correlations in *pure* 2D crystals at finite temperatures. A functional renormalization-group analysis in $d=4-\epsilon$ dimensions yields a nonuniversal exponent η that varies with the elastic constants of the FLL.[8,9] Extrapolating to $d=3$, one finds only a very weak variation with $1.143 < \eta < 1.159$.[8,9] Despite the glassy nature of the phase algebraically divergent Bragg peaks still exist which motivated the name Bragg glass.[6,7] The existence of the Bragg glass phase has been experimentally confirmed.[10,41]

After this summary of the scaling regimes, we briefly review the replica theory for the Hamiltonian of Eq. (1). Using the replica method, we average over point impurities (see

Appendix A) and obtain the replica Hamiltonian

$$\mathcal{H}_P^n = \sum_{\alpha=1}^n \mathcal{H}_0(\mathbf{u}^\alpha) - \frac{1}{2T} \sum_{\alpha,\beta=1}^n \int d^3\mathbf{r} R_P[\mathbf{u}^\alpha(\mathbf{r}) - \mathbf{u}^\beta(\mathbf{r})], \tag{13}$$

$$R_P(\mathbf{u}) = (v_p \rho_0)^2 n_{imp} \sum_{\mathbf{G} \neq 0} e^{i\mathbf{G}\mathbf{u}} \delta_{\xi^{-1}}(\mathbf{G}), \tag{14}$$

where $\delta_{\xi^{-1}}(\mathbf{G})$ is the delta function smeared out over a region of size ξ^{-1}. The correlation functions C_T and C_D that describe thermal fluctuations and disorder induced fluctuations, respectively, can be written as

$$C_T = \overline{\langle \tilde{\mathbf{u}}(\mathbf{q}) \tilde{\mathbf{u}}(-\mathbf{q}) \rangle} - \overline{\langle \tilde{\mathbf{u}}(\mathbf{q}) \rangle \langle \tilde{\mathbf{u}}(-\mathbf{q}) \rangle} = (2\pi)^d T \{ \tilde{\mathcal{G}}_L(\mathbf{q}) + \tilde{\mathcal{G}}_T(\mathbf{q}) \}$$

$$C_D = \overline{\langle \tilde{\mathbf{u}}(\mathbf{q}) \rangle \langle \tilde{\mathbf{u}}(-\mathbf{q}) \rangle} = (2\pi)^d \Delta(\mathbf{q}) \{ \tilde{\mathcal{G}}_L^2(\mathbf{q}) + \tilde{\mathcal{G}}_T^2(\mathbf{q}) \}, \tag{15}$$

where the last equation defines $\Delta(\mathbf{q})$, which we shell obtain in harmonic approximation below.

In Sec. III we study the interplay between point impurities and a planar defect. This is a difficult problem since we have to deal with two nonlinear terms. We consider the planar defect as a perturbation to the BG fixed point and examine the stability of the BG phase. Also we explore the effects of the defect on the order of the FLL. In the following we will use an effective quadratic Hamiltonian that reproduces the displacement correlations of Eq. (8) of the full nonlinear disordered model Eq. (13). A systematic analysis must be based on $\epsilon = 4-d$ expansion, and a functional renormalization-group analysis shows that displacements obey Gaussian statistics to lowest order in ϵ.[42] It should be noted that the effective Hamiltonian does not capture all physics, in particular, it cannot describe correctly the FL dynamics since it cannot reproduce the energy barriers for FL motion.[43] An effective quadratic Hamiltonian has been also used for a model with an uniaxial displacement to study a dislocation mediated transition of the FLL.[44]

The effective quadratic replica Hamiltonian in d dimensions reads[8,9]

$$\mathcal{H}_0^n = \frac{1}{2} \sum_{\alpha,\beta=1}^n (2\pi)^{-d} \int d^d\mathbf{q} \, \tilde{\mathbf{u}}^\alpha(\mathbf{q}) \tilde{\mathcal{G}}_{\alpha,\beta}^{-1}(\mathbf{q}) \tilde{\mathbf{u}}^\beta(-\mathbf{q}), \tag{16}$$

where

$$\tilde{\mathcal{G}}_{\alpha,\beta}^{-1}(\mathbf{q}) = \delta_{\alpha,\beta} \left(\tilde{\mathcal{G}}_L^{-1}(\mathbf{q}) \mathbf{P}_L + \tilde{\mathcal{G}}_T^{-1}(\mathbf{q}) \mathbf{P}_T + n \frac{\Delta(\mathbf{q})}{T} \mathbb{1} \right) - \frac{\Delta(\mathbf{q})}{T} \mathbb{1}. \tag{17}$$

It yields the correlation functions of Eq. (15), where $\Delta(\mathbf{q})$ describes the behavior of $\Delta = -\partial_{u_x}^2 R_P(\mathbf{0}) = -\partial_{u_y}^2 R_P(\mathbf{0})$ on different length scales. Using a functional renormalization group in $d=4-\epsilon$ dimensions, it has been shown that to lowest order in ϵ (Refs. 8 and 9),

$$\Delta(\mathbf{q}) \sim \begin{cases} 1, & \frac{1}{L_\xi} \lesssim q \lesssim \Lambda \\ q^{\epsilon - 2\zeta_{RM}}, & \frac{1}{L_a} \lesssim q \lesssim \frac{1}{L_\xi} \\ \epsilon q^\epsilon, & q \lesssim \frac{1}{L_a}. \end{cases} \quad (18)$$

The function $\Delta(\mathbf{q})$ reaches the fixed-point form $q^\epsilon \Delta^*(\kappa) c_{44} c_{66} a^2$ in the BG phase, where $\Delta^*(\kappa) \sim \epsilon/(1+\kappa)$ depends only on elastic constants but not on the disorder strength. We note that Emig et al.[8,9] obtained their results by calculating the integrals, needed for the RG equations, systematically for $d=4$ with a two-dimensional vector $\mathbf{z}$. The results are then extended to three dimensions by setting $\epsilon = 1$ in $\Delta^*(\kappa)$. This approach does not influence the main physics (like the logarithmic roughness of FL in the BG phase), but may influence the dependence of exponents η and ζ_{RM} on the elastic constants. In this way the dimensionality of z "axis" and the contribution of the term $c_{44} \mathbf{q}_z^2$ in the propagators are more weighted than the other axes and other terms $\sim c_{66}, c_{11}$, respectively. In the following, in order to not overestimate the effect of a planar defect that is parallel to the z axis, we will calculate all the integrals in $d=3$ if not stated otherwise. If the numerical values of η and ζ_{RM} are important for our conclusions, we will comment o n a possible influence that the use of results found by Emig et al.[8,9] can have.

III. SINGLE DEFECT

In this section the influence of a *single* planar defect on the Bragg glass order of the FLL is studied. In some parts of this section, when examining FLs density oscillations around the defect, we will study the isotropic limit with $c_{11}=c_{44} =c_{66}=c$ in order to focus on the important physics. In this limit the propagators read $\tilde{\mathcal{G}}_L^{-1}(\mathbf{q}) = \tilde{\mathcal{G}}_T^{-1}(\mathbf{q}) = cq^2$. By this assumption, only the weak dependence of η and ζ_{RM} on the elastic constants is ignored.

A. Model

The pinning energy of a planar defect can be written in the form

$$\mathcal{H}_D = \int d^3\mathbf{r}\, \rho(\mathbf{r}, \mathbf{u}) V_D(\mathbf{r} \cdot \mathbf{n}_D - \delta), \quad (19)$$

where $V_D(\mathbf{r} \cdot \mathbf{n}_D - \delta)$ is the potential of the defect plane. $\mathbf{n}_D$ and δ denote the unit vector perpendicular to the defect plane and its distance (along $\mathbf{n}_D$) from the origin of the coordinate system, respectively. The Bragg glass order that we are interested in is dominated by disorder fluctuations on large length scales where microscopic details become irrelevant. Therefore we may approximate the defect potential by a smeared out δ function, $V_D(x) \approx -v\, \delta_\xi(x)$. Since the superconducting order is reduced in the defect plane, it is plausible to assume $v > 0$ (for more details, see Sec. IX of Ref. 3). When we assume that FLs gain condensation energy when they overlap with the defect plane, a rough estimate for the defect
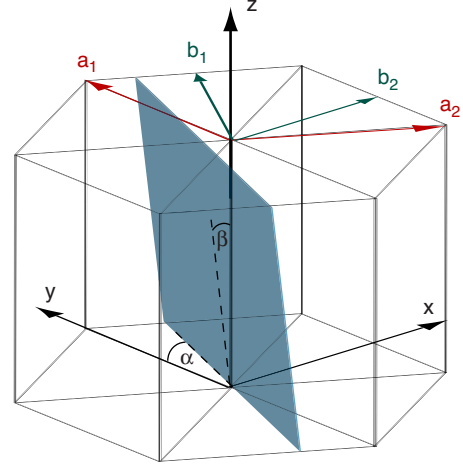

FIG. 2. (Color online) Vectors of the triangular flux-line lattice $(\mathbf{a}_1, \mathbf{a}_2)$ and of its reciprocal lattice $(\mathbf{b}_1, \mathbf{b}_2)$, and the angles α and β that define the orientation of the defect plane.

strength is $v \approx H_c^2 \xi^3$ with H_c the thermodynamic critical field.

In order to integrate over the delta function of the defect potential, it is convenient to introduce an explicit parametrization for the position vector $\mathbf{r}_D$ of the defect plane which obeys $\mathbf{r}_D \cdot \mathbf{n}_D = \delta$. With the parametrization

$$\mathbf{r}_D = (\mathbf{x}_D, z_D) + \delta \mathbf{n}_D, \quad z_D = t \cos\beta,$$

$$\mathbf{x}_D = (s \sin\alpha - t \cos\alpha \sin\beta, s \cos\alpha + t \sin\alpha \sin\beta),$$

$$\mathbf{n}_D = (\cos\beta \cos\alpha, -\cos\beta \sin\alpha, \sin\beta), \quad (20)$$

we introduce in-plane coordinates s and t, and the two angles α and β which determine the rotation of the plane with respect to the y and z axis, respectively (see Fig. 2). The defect energy now reads

$$\mathcal{H}_D = v\rho_0 \int dt\, ds\, dr_\perp\, \delta_\xi(r_\perp - \delta) \Bigg\{ \nabla_\mathbf{x} \mathbf{u}(t, s, r_\perp) - \sum_{\mathbf{G} \neq 0} e^{i\mathbf{G}[r_\perp \mathbf{n}_D + \mathbf{x}_D - \mathbf{u}(t,s,r_\perp)]} \Bigg\}, \quad (21)$$

where $r_\perp = \mathbf{r} \cdot \mathbf{n}_D$. Since the displacement field $\mathbf{u}$ varies slowly on the scale of the FLL constant a, the integrals over s and t vanish for all $\mathbf{G}$ with the exception of those for which the oscillatory factor $e^{i\mathbf{G}\mathbf{x}_D}$ is unity (for all s and t). This condition can be satisfied only if $\sin\beta = 0$, i.e., if the defect plane is *parallel* to the applied magnetic field. There remains a second condition for the angle α, which results from the constraint that $\mathbf{G} = m\mathbf{b}_1 + n\mathbf{b}_2$, with integer m and n, has to be perpendicular to $\mathbf{x}_D$. Expressing the defect plane (for $\beta=0$) as $\mathbf{x}_D = (c_1\mathbf{a}_1 - c_2\mathbf{a}_2)s$ where $\mathbf{a}_i\mathbf{b}_j = 2\pi\delta_{ij}$, one sees that the second condition is equivalent to the condition $m/n = c_2/c_1$. Hence if c_1/c_2 is irrational, the effect of the defect plane is always averaged to zero. On the other hand, for rational c_2/c_1 we may choose m_D, n_D to be the smallest coprime pair with $c_2/c_1 = m_D/n_D$. Then m_D and n_D are the Miller indices of the defect plane and only those $\mathbf{G}$ which are integer multiples of $\mathbf{G}_D = m_D\mathbf{b}_1 + n_D\mathbf{b}_2$ contribute in Eq. (21). In the fol-

lowing, we will concentrate on the contribution from these **G** vectors only. The FLL planes (of the ideal lattice) that are parallel to a defect plane with Miller indices m_D and n_D have a separation of $\ell = \frac{\sqrt{3}}{2}a/\sqrt{m_D^2 + m_D n_D + n_D^2}$ and hence $G_D = 2\pi/\ell$.

For the defect plane aligned to the magnetic field we take the x axis to be perpendicular to the defect (i.e., $\alpha = \beta = 0$), and hence the defect Hamiltonian becomes

$$\mathcal{H}_D = \rho_0 v \int dy\, dz \left\{ \boldsymbol{\nabla}_{\mathbf{x}} \mathbf{u}(\mathbf{r}_D) - \sum_{k>0}^{[\ell/\xi]_G} 2 \cos[kG_D(\delta - u_x)] \right\},$$

(22)

where $\mathbf{r}_D = (\delta, y, z)$. Here u_x denotes the component of the displacement field that is perpendicular to the defect plane and $[x]_G$ is the integer number that is closest to x.

B. Renormalization-group analysis

In this subsection we discuss the influence of the planar defect on the stability of the BG phase using a renormalization-group (RG) analysis. We employ a sharp-cutoff scheme by integrating out the displacement field $\tilde{\mathbf{u}}^>(\mathbf{q})$, with wave vectors $\mathbf{q}$ in an infinitesimal momentum shell below the cutoff $\Lambda > |\mathbf{q}| > \Lambda/b = \Lambda e^{-l}$ and subsequently rescale lengths and momenta according to

$$\mathbf{q}' = \mathbf{q}b,$$

(23)

$$\mathbf{r}' = \frac{\mathbf{r}}{b}.$$

(24)

We split the displacement field into weakly varying modes $\mathbf{u}^<(\mathbf{r})$ and strongly varying modes $\mathbf{u}^>(\mathbf{r})$ that include Fourier components out of and in the momentum shell, respectively. We choose to not rescale the field $\mathbf{u}'(\mathbf{r}') = \mathbf{u}^<(\mathbf{r})$, which implies a rescaling of its Fourier transform, $\tilde{\mathbf{u}}(\mathbf{q}') = \tilde{\mathbf{u}}^<(\mathbf{q})/b^3$.

The defect plane is considered as a perturbation to the Hamiltonian of Eq. (16). The gradient term of Eq. (22) scales $\sim L$ if the defect size $\sim L^2$. Since the elastic energy Eq. (2) scales in the same way, the gradient term is a marginal perturbation. It can be also eliminated by the transformation $u_x'(\mathbf{r}) = u_x(\mathbf{r}) + \frac{v\rho_0}{2c_{11}}\text{sgn}(x - \delta)$, where $\text{sgn}(0) = 0$. This transformation does neither change the terms $\sim c_{66}$ and c_{44} of Eq. (2) nor the pinning energy due to point impurities in Eq. (13) since all replica fields are transformed in the same way. The gradient term of the defect pinning energy tends to increase the FL density at the defect as can be seen from the transformation above.

In order to account for different renormalization of the harmonic components of the defect pinning energy, we introduce the variables v_k for the strengths of the harmonics of order k. A cumulant expansion yields to first order in v the renormalization

$$\frac{v_k(l)}{T(l)} = \frac{v}{T}e^{2l}\langle \cos[kG_D u_x^{\alpha,>}(\mathbf{r}_D)] \rangle$$

$$= \frac{v}{T}e^{2l}e^{-\frac{1}{2}(kG_D)^2\langle[u_x^{\alpha,>}(\mathbf{r}_D)]^2\rangle}$$

$$= \frac{v}{T}e^{(2-k^2 g)l}, \quad g = \frac{3}{8}\eta\left(\frac{a}{\ell}\right)^2,$$

(25)

where the factor e^{2l} is due to a rescaling of lengths. $\langle[u_x^{\alpha,>}(\mathbf{r}_D)]^2\rangle$ is obtained at the BG fixed point to linear order in l. Due to the irrelevance of thermal fluctuations, we have neglected contributions that come from the thermal part of the propagator of Eq. (17). We have chosen to rescale temperature instead of elastic constants in order to organize the RG analysis of the zero-temperature BG fixed point. It is important to note that Eq. (25) holds only on length scales larger than the positional correlation length L_a.

In the random manifold regime $\overline{\langle e^{i\mathbf{G}\mathbf{u}(\mathbf{r})}\rangle}$ decays with the system size as a stretched exponential and the effect of the defect plane is reduced by disorder fluctuations on intermediate length scales. Hence, the renormalized and rescaled value of the defect strength is reduced to

$$v_k \approx v(L_a/a)^2 e^{-\mathcal{C}(G_D k a)^2}$$

(26)

on the scale $L = L_a$, where $\mathcal{C}$ is a positive constant. This value is the initial defect strength $v_k(l=0)$ to be used in Eq. (25).

The RG flow equations in the Bragg glass regime now read

$$\frac{dT}{dl} = -T,$$

(27)

$$\frac{dv_k}{dl} = v_k(1 - k^2 g).$$

(28)

Hence v_1 is a relevant perturbation provided $g < 1$, i.e., if

$$\eta(m_D^2 + m_D n_D + n_D^2) < 2 \quad \text{or} \quad \ell > \sqrt{\frac{3\eta}{8}}a \approx 0.66\ a,$$

(29)

which is compatible only with $\ell = \sqrt{3}a/2 \approx 0.87a$. A relevant defect plane must be oriented parallel to one of the three main crystallographic planes of the FLL (i.e., $\cos 2\beta = \cos 6\alpha = 1$). When ℓ increases (g decreases) more FLs can gain energy from the defect plane and hence render it more relevant.

Emig et al.[8,9] calculated η in a one-loop functional RG expansion in $4-\epsilon$ dimensions. Higher loops as well as the fact that all integrals are evaluated in $d=4$ with **z** being a two-dimensional vector may influence the actual numerical value of the coefficient η in $d=3$. However, we argue that this higher-order correction does not affect our conclusion that a single defect is relevant only if it is parallel to the main crystallographic planes since $g = \eta(m_D^2 + m_D n_D + n_D^2)/2$ can change only in finite steps ($\eta/2, 3\eta/2, 7\eta/2, \dots$) when rotating the defect plane (see Fig. 3).
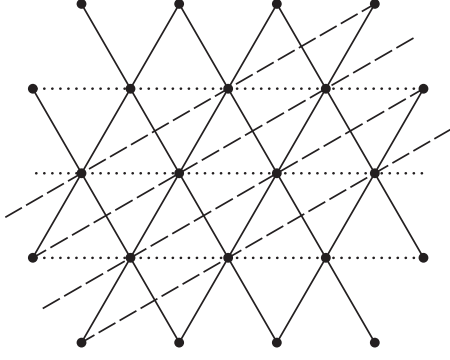
FIG. 3. Two possible orientations of defect planes relative to the flux-line lattice, corresponding to $g = \eta/2$ (dotted lines) and $3\eta/2$ (dashed lines).

C. Effective Hamiltonian

In this section we discuss whether higher order cumulants in v can lead to a renormalization of the parameter g and hence can influence the condition for the relevance of a defect that was derived in Sec. III B. The renormalization described by Eq. (28) does not occur in the bulk but on the defect plane. Hence it is possible to develop an effective theory that is defined on the defect plane only. Since the defect couples only to the displacement u_x on the defect plane, we integrate out u_x outside the defect and u_y across the entire sample. This integration is facilitated by employing the effective Gaussian theory for the BG phase of Sec. III B. At $T = 0$ we are interested in the ground state and hence we solve the Euler-Lagrange equation for $\mathbf{u}(\mathbf{r})$ with the condition $u_x(\mathbf{r}_D) = \varphi(\mathbf{r}_D)$ at the defect plane, where $\varphi(\mathbf{r}_D)$ is an arbitrary function. An equivalent functional-integral approach is presented in Appendix B. The effective replica Hamiltonian on the defect plane reads

$$\mathcal{H}_{eff}^n = -\sum_\alpha \sum_{k>0} 2v_k \rho_0 \int d\mathbf{r}_D \cos\{kG_D[\delta - \varphi^\alpha(\mathbf{r}_D)]\}$$
$$+ \frac{1}{2} \sum_{\alpha,\beta} \frac{1}{(2\pi)^{d-1}} \int d^{d-1}\mathbf{q}\, \tilde{\varphi}^\alpha(\mathbf{q}) \tilde{\mathcal{Q}}_{\alpha,\beta}^{-1}(\mathbf{q}) \tilde{\varphi}^\beta(-\mathbf{q}),$$
$$(30)$$

where $\mathbf{q}$ is the in-plane momentum,

$$\langle \tilde{u}_x^\alpha(x,\mathbf{q}) \tilde{u}_x^\beta(x,\mathbf{q}') \rangle = T(2\pi)^d \delta(\mathbf{q}+\mathbf{q}') \tilde{\mathcal{Q}}^{\alpha,\beta}(\mathbf{q}), \quad (31)$$

and v_k are renormalized parameters on the scale of the positional correlation length. In order to avoid technical complications, we consider the limit of isotropic elasticity. In line with an ϵ expansion, we evaluate the integrals in $d=4$ and then set $\epsilon=1$ in the expression for fixed-point value $\Delta^*(\kappa)$. This approach does not affect our conclusion and leads to a clearer result. On scales larger than L_a we get

$$\mathcal{Q}_{\alpha,\beta}^{-1}(\mathbf{q}) = 2 \sqrt{\frac{cn\Delta_{BG}}{T} + (qc)^2}\, \delta_{\alpha,\beta}$$
$$- \frac{2c\Delta_{BG}}{T}\left(cq + \sqrt{\frac{cn\Delta_{BG}}{T} + (qc)^2}\right)^{-1}, \quad (32)$$

where c is the elastic constant and $\Delta_{BG} = c^2 a^2 \Lambda \Delta^*(1)$. The same procedure can be performed also in the RF and RM regimes using the corresponding quadratic Hamiltonian in d dimensions. The effective Hamiltonian in $d-1$ dimensions has a long-ranged elasticity (term $\sim q$ in the limit $\Delta_{BG} \to 0$) that results from the local bulk elasticity. A RG analysis of the effective Hamiltonian of Eq. (30) shows that neither Δ_{BG} nor the elastic constants are renormalized, and hence g is not renormalized. From this we conclude that a weak defect is a relevant perturbation only for $g < 1$.

D. Density oscillations

Next, we study the order of the FLs next to a defect plane. We consider separately the case of a relevant and an irrelevant planar defect plane. For simplicity, we assume isotropic elasticity and choose to place the origin of the coordinate system on the defect plane, i.e., wet set $\delta = 0$. In the absence of a planar defect, FL density fluctuations due to point impurities obey $\overline{\langle \rho(\mathbf{r}) - \rho_0 \rangle} = 0$. The defect plane pins FLs and yields a *long-ranged* restoration of the translational order parameter $e^{i\mathbf{G}\mathbf{u}(\mathbf{r})}$. We find Friedel-type oscillations of the FL density with an amplitude that decays as a power law with an exponent that depends on if the defect is relevant or irrelevant in the RG sense.

1. Irrelevant defect

First, we consider an irrelevant defect parallel to the magnetic field. The irrelevance of the defect potential for $g > 1$ allows us to compute the thermal and disorder average of FL density perturbatively in the defect strength,

$$\overline{\langle \delta\rho[\mathbf{r}, \mathbf{u}(\mathbf{r})] \rangle} = \lim_{n\to 0} \prod_{\alpha=1}^n \int \mathcal{D}\mathbf{u}^\alpha \delta\rho[\mathbf{r}, \mathbf{u}^\gamma(\mathbf{r})] e^{-\beta\mathcal{H}^n}, \quad (33)$$

where $\delta\rho(\mathbf{r},\mathbf{u}) = \rho(\mathbf{r},\mathbf{u}) - \rho_0$, γ is an arbitrary replica index, and

$$\mathcal{H}^n = \mathcal{H}_0^n + \sum_\alpha \mathcal{H}_D(\mathbf{u}^\alpha). \quad (34)$$

To lowest order in the defect strength we get

$$\overline{\langle \delta\rho[\mathbf{r}, \mathbf{u}(\mathbf{r})] \rangle} = \lim_{n\to 0} \langle \delta\rho[\mathbf{r}, \mathbf{u}^\gamma(\mathbf{r})] \rangle = 0. \quad (35)$$

Even if the defect is irrelevant in the RG sense, it breaks the translational symmetry perpendicular to the defect and hence modifies the FL density locally. To correctly describe this effect we need to compute the average change in the FL density to first order in v.

$$\overline{\langle \delta\rho[\mathbf{r}, \mathbf{u}(\mathbf{r})] \rangle} = -\beta \lim_{n\to 0} \sum_{\alpha=1}^n \langle \delta\rho[\mathbf{r}, \mathbf{u}^\gamma(\mathbf{r})] \mathcal{H}_D(\mathbf{u}^\alpha) \rangle. \quad (36)$$

We find that in the limit $T \to 0$ this result can be expressed as

$$\overline{\langle \delta\rho[\mathbf{r},\mathbf{u}(\mathbf{r})]\rangle} \approx \frac{v_1\rho_0^2 G_D^2 L_a}{c(2g-1)} \cos(G_D|x|) \left(\frac{L_a}{|x|}\right)^{2g-1}, \quad (37)$$

which becomes exact for large x, see Appendix C. The result captures the large length scale behavior for $L \gtrsim L_a$. Here v_1 denotes the effective defect strength on the scale L_a, cf. Eq. (26), and $|x|$ is the normal distance from the defect plane. There are additional contributions to Eq. (37) coming from the higher harmonics in $\mathcal{H}_D$. They are less important since they are proportional to v_k on the scale L_a and they decay as $|x|^{-2k^2g+1}$ with $k \geq 2$. Although the defect is irrelevant in RG sense, it leads to Friedel-type oscillations in the density.

If the defect plane is *not* parallel to the applied magnetic field, Friedel oscillations occur as well. However, the amplitude is exponentially suppressed. The amplitude of density oscillations with reciprocal-lattice vectors $\mathbf{G} = G(\cos\alpha, -\sin\alpha)$ (for a definition of the angles α and β see Fig. 2) decays beyond the distance $1/(G|\sin\beta|)$ from the defect plane. Similar physics occur in classical two-dimensional systems with a columnar defect.[28,29]

2. Relevant defect

The strength of a relevant defect grows under renormalization relative to the elastic and the impurity energy. On the scale

$$L_v \approx \max\left\{ L_a, L_a\left(\frac{ca^4}{vL_a}\right)^{1/(1-g)} \right\}, \quad (38)$$

the energies become of the same order and perturbation theory breaks down. On larger scales, the defect potential can be described effectively through the boundary condition $u_x(x=0,y,z)=0$ for the displacement field at the defect plane. With this constraint the system gains maximal energy from the defect and the complete energy of the system is minimized. First, we calculate displacement correlations $\mathcal{G}_{pin,ij}(x,x';\mathbf{r}_\parallel - \mathbf{r}'_\parallel) = T^{-1}\overline{\langle u_i(\mathbf{r})u_j(\mathbf{r}')\rangle}$ with the above boundary condition at the defect and $\mathbf{r}=(x,\mathbf{r}_\parallel)$. We find in momentum space (see Appendix D)

$$\tilde{\mathcal{G}}_{pin,ij}(x,x;\mathbf{q}) = \lim_{n\to 0}\Big[\tilde{\mathcal{G}}_{ij}^{11}(0,\mathbf{q}) - \sum_{\alpha\gamma}\tilde{\mathcal{G}}_{ix}^{1\alpha}(|x|,\mathbf{q})\tilde{\mathcal{Q}}_{\alpha,\gamma}^{-1}(\mathbf{q})$$

$$\times\tilde{\mathcal{G}}_{xj}^{1\gamma}(|x|,-\mathbf{q})\Big], \quad (39)$$

where $\mathbf{q}$ is the in-plane momentum and $\tilde{\mathcal{G}}^{\alpha,\beta}$ is the inverse of $\tilde{\mathcal{G}}_{\alpha,\beta}^{-1}$ given by Eq. (17). i,j stand for x,y and $\mathcal{Q}$ is given by Eq. (31). It can be shown that the displacement correlations on scales larger than L_v are given by

$$\overline{\langle u_i(\mathbf{r})u_j(\mathbf{r})\rangle} = \lim_{n\to 0} T[\mathcal{G}_{ij}^{11}(0,\mathbf{0}) - (\hat{\mathbf{x}}\cdot\hat{\mathbf{i}})(\hat{\mathbf{x}}\cdot\hat{\mathbf{j}})\mathcal{G}_{xx}^{11}(2|x|,\mathbf{0})].$$

$$(40)$$

Using this result, we obtain for the average change in the FL density

$$\overline{\langle \delta\rho(\mathbf{r},\mathbf{u}(\mathbf{r}))\rangle} = 2\rho_0\sum_{m>0}\cos(mG_Dx)\left(\frac{L_v}{|x|}\right)^{m^2g}. \quad (41)$$

These oscillations resemble Friedel oscillations which can be also found in Luttinger liquids with an isolated impurity[32] or in classical two-dimensional systems with a columnar defect.[28,29]

The amplitude of the Friedel oscillations decays as a power law with an exponent g and $2g-1$ for a relevant and an irrelevant defect, respectively. For an irrelevant defect the amplitude decays more rapidly than for a relevant defect. In the absence of point impurities the defect is always relevant in the RG sense, and the amplitude of the Friedel oscillations remains finite for $|x| \to \infty$.

IV. FINITE DENSITY OF WEAK DEFECTS

A. Model

In this section we consider a finite density of parallel planar defects with *random position*. We assume that defects extend along the entire sample and are aligned parallel to the applied magnetic field. There is a competition between the two random potentials from planar defects and point impurities. The defects tend to localize the FLs and hence favor order along the defect planes while point impurities promote FL wandering.

The Hamiltonian reads

$$\mathcal{H} = \mathcal{H}_0 + \int d^3r[V_P(\mathbf{r}) + V_D(\mathbf{r})]\rho(\mathbf{r},\mathbf{u}), \quad (42)$$

where $\mathcal{H}_0$ is the elastic Hamiltonian of Eq. (2) and V_P is the pinning potential resulting from point impurities [see Eq. (5)]. The defect pinning potential is $V_D(\mathbf{r})=-v\{\sum_i\delta_\xi(x-x_i) -1/\ell_D\}$, where we assumed that the defect planes are parallel to the yz plane and ℓ_D is a mean defect spacing. The δ function is assumed to have a finite width of the order of the superconductor coherence length ξ. The defect potential is uncorrelated along the x axis,

$$\overline{V_D(\mathbf{r}_1)V_D(\mathbf{r}_2)} = \frac{v^2}{\ell_D}\delta_\xi(x_1-x_2). \quad (43)$$

We discuss the case where the gap between two defect planes typically contains many FLs, i.e., $\xi \ll \ell \ll \ell_D$. Note that orientation of the defects is otherwise arbitrary.

After averaging over the defect positions, the replica Hamiltonian for the defects reads

$$\mathcal{H}_D^n = -\frac{(v\rho_0)^2}{2T\ell_D}\int d^3\mathbf{r}_1 d^3\mathbf{r}_2\sum_{\alpha,\beta}\delta_\xi(x_1-x_2)$$

$$\times\Big\{ -2\nabla_\mathbf{x}\mathbf{u}^\alpha(\mathbf{r}_1)\sum_\mathbf{G}e^{i\mathbf{G}[\mathbf{x}_2-\mathbf{u}^\beta(\mathbf{r}_2)]} + \nabla_\mathbf{x}\mathbf{u}^\alpha(\mathbf{r}_1)\nabla_\mathbf{x}\mathbf{u}^\beta(\mathbf{r}_2)$$

$$+\sum_{\mathbf{G}_1,\mathbf{G}_2}e^{i\mathbf{G}_1[\mathbf{x}_1-\mathbf{u}^\alpha(\mathbf{r}_1)]}e^{i\mathbf{G}_2[\mathbf{x}_2-\mathbf{u}^\beta(\mathbf{r}_2)]}\Big\}, \quad (44)$$

where $\mathbf{x}=(x,y)$. The defects are assumed to be sufficiently weak so that terms of the order v^3/ℓ_D and higher can be neglected. The first term does not contribute to $\mathcal{H}_D^n$ due to the

oscillatory factor $e^{i\mathbf{G}x_2}$ and the third term contributes only for reciprocal vectors perpendicular to the defects satisfying $\mathbf{G}_1 = -\mathbf{G}_2 = n\mathbf{G}_D$ with integer n. Introducing the relative coordinate $x_r = x_1 - x_2$ and taking into account that $\delta_\xi(x_r)$ is finite for $|x_r| \lesssim \xi$, we approximate the displacement field as $u_x(x_2 + x_r, y_1, z_1) \approx u_x(x_2, y_1, z_1)$. This approximation is justified since the displacement field varies slowly over the FL spacing. Then Eq. (44) can be written as

$$\mathcal{H}_D^n = -\frac{1}{2T} \int_{x_1, y_1, z_1, y_2, z_2} \sum_{\alpha, \beta} \{ \sigma \boldsymbol{\nabla}_\mathbf{x} \mathbf{u}^\alpha(x_1, y_1, z_1) \boldsymbol{\nabla}_\mathbf{x} \mathbf{u}^\beta(x_1, y_2, z_2)$$
$$+ R_D[u_x^\alpha(x_1, y_1, z_1) - u_x^\beta(x_1, y_2, z_2)] \}, \qquad (45)$$

where

$$R_D(u_x) = \sigma \sum_{n \neq 0} \delta_{\xi^{-1}}(nG_D) e^{inG_D u_x} \qquad (46)$$

and we defined $\int_x = \int dx$ and $\sigma = (v\rho_0)^2/\ell_D$. After averaging over point impurities, the complete replica Hamiltonian is $\mathcal{H}^n = \mathcal{H}_P^n + \mathcal{H}_D^n$, where $\mathcal{H}_P^n$ is given by Eq. (13).

The first term in Eq. (45) comes from the coupling of the defect potential to the slowly varying part of the FL density $\sim \boldsymbol{\nabla}_\mathbf{x} \mathbf{u}$. This term does not contribute to the glassy properties of the system since it can be eliminated by a simple transformation.[43,45] (For a more detailed discussion of this term see below.) The remaining part of the replica pinning energy $\mathcal{H}^n$ is invariant under the transformations

$$u_x^\alpha(\mathbf{r}) \rightarrow u_x^\alpha(\mathbf{r}) + f_x(x), \qquad (47)$$

$$u_y^\alpha(\mathbf{r}) \rightarrow u_y^\alpha(\mathbf{r}) + f_y(\mathbf{r}), \qquad (48)$$

where $f_x(x)$ and $f_y(\mathbf{r})$ are arbitrary functions. Equation (47) represents an approximate symmetry if the defect potential has a finite width. However, with increasing length scale, deviations from the symmetry become less important. These symmetries show that the elastic coefficient c_{11} is not renormalized. Not renormalized are also the elastic moduli which determine the energy cost for tilting the FLs *only* in the y direction [i.e., the term $c_{44}(\partial_z u_y)^2$] and for changing only the displacement u_y along the x axis [i.e., the term $c_{66}(\partial_x u_y)^2$]. These symmetries are commonly denoted as statistical tilt symmetry.[46] However, the defects are an important source of anisotropy and other elastic properties of the FLL will be affected. For example, the energy cost for FL tilting as well as FLL shearing parallel and perpendicular to the planes will differ considerably. Also, due to the defect planes the system is not invariant under arbitrary rigid rotations of the FLL around z axis and rotational modes will appear in the elastic Hamiltonian under renormalization.[47] Note that for the FLL with point disorder only, none of the elastic constants will be renormalized since the disorder correlation function $R_P(\mathbf{u})$ is invariant under the more general transformation $\mathbf{u}^\alpha(\mathbf{r}) \rightarrow \mathbf{u}^\alpha(\mathbf{r}) + \mathbf{f}(\mathbf{r})$.

Planar defects in the form of twin boundaries that are perpendicular to the copper oxide planes very often appear in YBa$_2$Cu$_3$O$_{7-x}$ (YBCO).[16,17,19] YBCO is a high-temperature superconductor and within high accuracy it is uniaxially anisotropic.[3] YBCO can be reasonably well described within a continuum anisotropic model, while for more strongly layered superconductors a different description is needed. The elastic description for anisotropic superconductors can be found in the review article in Ref. 3. The number of independent elastic moduli increases with respect to the isotropic case that we discussed in Sec. II. However, if the magnetic field is applied perpendicular to the copper oxide planes, the model given by Eq. (2) as well as the considerations in the following sections is directly applicable also for YBCO.

B. Functional renormalization-group approach

In Sec. IV A we treated a single defect plane as a perturbation to the Bragg glass fixed point. Now, we consider both the planar defects and the point impurities as a perturbation to the ideal Shubnikov phase. Notice that Eq. (46) depends only the displacement field u_x. Since we focus below on the effect of the defect planes, it seems to be justified to start from a simplified model in which only the displacement $u_x \equiv u$ of the FLs *perpendicular* to the defect planes is considered. This model describes also a wide class of other systems which exhibit regular lattices of domain walls such as magnets, charge-density waves,[33] and incommensurate systems.[34]

In the absence of the defect planes point impurities are relevant below four dimensions. We employ here an Imry-Ma-type argument[48] in combination with perturbation theory to see the effect of randomly distributed point impurities on the FLL. When the initially ordered FLL is distorted in a volume L^d by $u \sim \ell$, the typical energy gain is of the order $\sim [-R_P''(0)L^d]^{1/2}$ compared to the elastic energy loss $\sim L^{d-2}$. For $d < d_P = 4$ and sufficiently large $L \gg L_\xi \sim [-R_P''(0)]^{1/(d-4)} \gg \ell$ the point disorder wins and the FLL becomes distorted. A more detailed study shows that in this case the FLL exhibits a phase with quasi long-range order, which is the previously discussed Bragg glass phase (see Sec. II). In this phase the positional correlation function $S_\mathbf{G}$ [see Eq. (9)] shows a power-law decay.

Next we consider the Imry-Ma argument for planar defects in a volume $L_x^{d-2} L_z L_y$ without point impurities. The energy gain is of the order $[-R_D''(0)\ell^2 L_x^{d-2}]^{1/2} L_z L_y$. The elastic energy loss is $c_{11} L_z L_y L_x^{d-4} \ell^2$ since distortions are aligned parallel to the defects. For $L_x \gg L_D \sim [-c_{11}^2 \ell^2/R_D''(0)]^{1/(6-d)}$ the pinning energy gain wins and the FLL becomes disordered in the direction perpendicular to the defects. L_D is the so-called Larkin length for the defects. The critical dimension above which weak planar defects are irrelevant is $d_D = 6$.

For an RG approach is convenient to consider a generalization of our model to d dimensions. The defects remain two dimensional with $d-2$ transverse directions, while the displacement field remains uniaxial. In the following, we use a functional RG approach[49,50] in $d = 6 - \epsilon$ dimensions. We follow closely a related approach for columnar disorder[51,52] but do not rescale the renormalized quantities so that they correspond to the effective parameters measured on the scale L_x. Thermal fluctuations and point disorder are irrelevant for $\epsilon < 4$ and $\epsilon < 2$, respectively. Hence we can assume directly $T = 0$ and $R_P = 0$. To lowest order in ϵ the RG flow equation read

$$\frac{d \ln c_{ii}}{d \ln L_x} = \frac{K_d R_D''''(0) L_x^\epsilon}{c_{11}^2}, \quad i = 4, 6, \qquad (49)$$

$$\frac{dR_D(u)}{d \ln L_x} = \frac{K_d R_D''(u) L_x^\epsilon}{2c_{11}^2}[R_D''(u) - 2R_D''(0)], \qquad (50)$$

where $K_d = S_{d-2}/(2\pi)^{d-2}$ and S_d denotes the surface of the d-dimensional unit sphere.

In a static situation the displacement field is independent on y and z since defects distort FLL planes that are parallel to the yz plane on the whole. Since, by assumption, other sources of fluctuations are not present we can perform the integration over y and z in the Hamiltonian of Eq. (45) and obtain an effective $d-2$ dimensional Hamiltonian that describes the interaction of FLL planes with defect planes with $d-2$ dimensional random positions. This explains why the flow equation for R_D has the form as the one for the point disorder correlator R_P in $d-2$ dimensions.[6] However, an important difference between the d-dimensional FLL with defects and the FLL planes with point impurities in $d-2$ dimensions is the renormalization of elastic constants c_{44} and c_{66} in the former model.

For $L_x \to L_D$, $R_D''''(0)$ increases and at $L_x \approx L_D$ $R_D''(u)$ develops a cusp at $u=0$. The cusp signals the appearance of metastable states the energy of which is very close to the ground-state energy but which may be far apart in configuration space. The cusp results in diverging elastic constants c_{44} and c_{66} and in a change of the sign of $R''''(0^+)$ from positive to negative. If there is a small but finite tilt or shear of FLs, $R_D''''(0)$ has to be replaced by $R''''(0^+)$ in Eq. (49), and on length scales $L_x > L_D$ the elastic constants decrease since $R''''(0^+)$ is then negative. Importantly, a new term of the form

$$\frac{1}{\ell} \int d^{d-2}x dy dz |\Sigma_y(\partial_y u)\hat{y} + \Sigma_z(\partial_z u)\hat{z}| \qquad (51)$$

is generated in the Hamiltonian. $\Sigma_{z(y)}$ has the meaning of an interface tension of a domain wall perpendicular to z (y) axis, across which the displacement field changes by ℓ. They dominate the elastic energy for small u and are renormalized according to

$$c_{66}^{-1/2}\frac{d\Sigma_y}{d \ln L_x} = c_{44}^{-1/2}\frac{d\Sigma_y}{d \ln L_x} = R_D'''(0^+)L_x^{5-d}\frac{K_d \ell}{2c_{11}^{3/2}}. \qquad (52)$$

Σ_z and Σ_y satisfy the relation $\Sigma_z/\Sigma_y = \sqrt{c_{44}}/\sqrt{c_{66}}$. Notice that c_{44} and c_{66} are renormalized in the same way such that their ratio remains constant under the RG flow.

Next we estimate the Larkin length L_D from the flow equations. The function $R_D(u)$ is even and as long as it is analytic, all odd derivatives at $u=0$ vanish. Assuming analyticity, the flow equation for $R_D''''(0)$ reads

$$\frac{dR_D''''(0)}{d \ln L_x} = \frac{4}{c_{11}^2}K_d L_x^\epsilon[R_D''''(0)]^2. \qquad (53)$$

The solution on the length scale L_x is given by $R_D''''(0,L_x) = R_D''''(0,\lambda)[1 - R_D''''(0,\lambda)4K_d(L_x^\epsilon - \lambda^\epsilon)/c_{11}^2\epsilon]^{-1}$, where λ is the penetration depth and has a role of the small length scale cutoff. This shows that $R_D(0)$ diverges at

$$L_D \approx \left[\frac{\epsilon c_{11}^2}{4K_d R_D''''(0,\lambda)}\right]^{1/\epsilon}. \qquad (54)$$

This result is in qualitative agreement with the estimate we obtained from scaling arguments since $R_D''''(0,\lambda)\ell^2 \sim R_D''(0,\lambda)$.

The fixed-point function has for $0 \le u < \ell$ the form[6]

$$R_D^{*''}(u,L_x) = -\frac{\epsilon c_{11}^2 L_x^{-\epsilon}}{6K_d}\left[\left(u - \frac{\ell}{2}\right)^2 - \frac{\ell^2}{12}\right] \qquad (55)$$

and it has to be periodically continued in u with period ℓ. Note that if we would consider rescaled quantities then in Eq. (55) $L_x^{-\epsilon}$ would be replaced by Λ^ϵ. In the case of a finite tilt (shear) for $L_x > L_D$ the elastic constant c_{44} (c_{66}) decreases as $c_{ii}(L_x) \sim (L_x/L_D)^{-\epsilon/3}$. A rough estimate for the saturation value for the interface tension is $\Sigma_z \sim \epsilon \ell^2 \sqrt{c_{11}c_{44}(\lambda)}/L_D$.

As has been pointed out by Fedorenko,[52] the RG equations for the elastic constants c_{44} and c_{66} and the interface tensions resemble those of the friction and driving force for the depinning transition of the FLL in the presence of point impurities.[53] The role of velocity is here played by tilt or shear and the elastic constants diverge at zero tilt and zero shear as the friction diverges in the static case. Also, as a threshold force exists for the depinning transition, the interface tension $\Sigma_{z(y)}$ determines the threshold force for tilting (shearing) the FLL, as we will see in Sec. IV C.

C. Properties of the planar glass

In this subsection we summarize the properties of the new phase that is described by the fixed point of the functional RG of the previous section and in the following is called "planar glass." We examine the response of the system to FL tilting, to a change in the longitudinal magnetic field and discuss the order of the FLL. We show that the new phase and its properties are robust against weak point impurities in $d=3$ and $d=4$.

When one changes the direction of the applied magnetic field by $H_x\hat{x}$, the Hamiltonian changes by

$$\delta\mathcal{H} = -\frac{\phi_0\rho_0}{4\pi}\int d^3r H_x \partial_z u. \qquad (56)$$

To tilt the FLs with respect to the z axis, H_x has to overcome the interface energy $\sim \Sigma_z$, which results in a threshold field

$$H_{x,c} = 2\pi\sqrt{3}\frac{\Sigma_z a^2}{\phi_0\ell}, \qquad (57)$$

below which the FLs remain locked parallel to the planes. This is the *transverse Meissner effect*: a weak transverse magnetic field H_x is screened from the sample and c_{44} is infinite. Only for $H_x > H_{x,c}$ the average tilt of the FLs becomes nonzero and c_{44} is finite. In this way, by measuring the threshold field, Σ_z can be measured.

Moreover, there is a *resistance against shear* of the FLL. The shear deformation $\partial_y u_x$ is nonzero (and c_{66} is finite) only if the shear stress σ_{xy} is larger than a critical value $\sigma_{xy,c} = \Sigma_y/\ell$. Otherwise c_{66} is infinite. The divergence of c_{66} is a new property that does not appear in the Bose glass which,

however, does also show a transverse Meissner effect.

An infinitesimal change in the longitudinal magnetic field $\delta H_z \hat{\mathbf{z}}$ changes the Hamiltonian by

$$\delta \mathcal{H} = -\frac{\phi_0 \rho_0}{4\pi} \int d^3 r \, \delta H_z \partial_x u \quad (58)$$

and allows to measure the longitudinal magnetic susceptibility $\chi = \phi_0 \rho_0 \partial \langle \partial_x u \rangle / \partial \delta H_z$. The disorder averaged susceptibility is

$$\bar{\chi} = \frac{(\phi_0 \rho_0)^2}{4\pi c_{11}}, \quad (59)$$

as shown in Appendix E. It is independent of disorder as a result of the statistical tilt symmetry.[46] The glassy properties of the system can most easily be seen by the sample-to-sample fluctuations of the magnetic susceptibility. Perturbation theory yields (see Appendix E)

$$\frac{\overline{\chi^2} - \bar{\chi}^2}{\bar{\chi}^2} = \frac{R_D''''(0) L_x^\epsilon}{5 c_{11}^2} \sim \left(\frac{L_x}{L_D}\right)^\epsilon, \quad (60)$$

i.e., the sample-to-sample fluctuations of the susceptibility grow with the scale $L_x \lesssim L_D$, $d < 6$. We cannot expect that this result is quantitatively correct for large L_x, but qualitatively it demonstrates the relevance of defects and it provides a signature of a glassy phase.[43] Although we were not able to prove it, $\overline{\chi^2}/\bar{\chi}^2 - 1$ will most likely approach a finite universal value for $L_x \gg L_D$ in $d < 6$.

The positional correlation function is obtained to first order in perturbation theory, combined with a functional RG analysis for $6 > d > 4$. It reads

$$S_{\mathbf{G}_D}(x,y,z) \sim |\mathbf{x}|^{-\eta_D}, \quad (61)$$

where $\eta_D = (\pi/3)^2(6-d)$. A detailed derivation of this result is presented in Appendix F. In order to study the behavior in $d \leq 4$, we have to reconsider the first term of Eq. (45). It results from the coupling of the defect potential to the slowly varying part of the FL density ($\sim \partial_x u$). By taking into account that at a scale L_x the displacement field behaves as $u \sim L_x^\zeta$, we find that the σ term scales as $\sim L_y^2 L_z^2 L_x^{d-4+2\zeta}$. When we compare the latter term to the squared elastic Hamiltonian $\sim L_y^2 L_z^2 L_x^{2(d-4+2\zeta)}$ that describes the cost of deviations of u in the $\mathbf{x}$ directions only (since the FLs are completely ordered parallel to the defects on sufficiently large scales in the absence of point impurities), we find that the σ term becomes relevant if $d - 4 + 2\zeta \leq 0$. For logarithmic roughness ($\zeta = 0$) it is relevant for $d \leq 4$. Since the other part of the defect pinning energy $\sim R_D(u)$ scales in the same way as the elastic energy, the σ term is the dominant part of the pinning energy and determines the FL roughness.

First, we consider the case without point impurities and then treat them perturbatively. Applying a Flory-type argument,[54] i.e., assuming that the elastic energy and the dominant part of the defect energy scale in the same way, we find, following the discussion above, that in $d = 3$ the roughness exponent is $\zeta = 1/2$. More detailed calculations[55,56] confirm our result, leading to

$$S_{\mathbf{G}_D}(x,y,z) \sim e^{-|x|/\xi_c}, \quad (62)$$

where $\xi_c \approx L_D$. Note that there is a shift of dimension $d \to d + 2$ between the model studied in Refs. 55 and 56 to our model since the FLs are ordered in the yz plane. In Refs. 55 and 56 a related one-dimensional system with point impurities at zero temperature is studied. There is a nontrivial renormalization of σ coming from the defect potential that couples to the periodic part of the FL density.[55] The σ term does not contribute to the renormalization of R_D since the σ term can be eliminated in every step of the RG procedure by applying the transformation that does not affect the correlator R_D, as discussed at the beginning of this section. That is why Σ_z and Σ_y will be generated also for $d \leq 4$. Villain and Fernandez[55] found from a nonperturbative RG that for $d \leq 4$ the defect-induced disorder flows under the RG to strong coupling. However, our study of the strong-coupling limit in Sec. IV shows that this limit gives qualitatively the same result as the case investigated in this section.

To summarize, the planar glass phase is characterized by (i) diverging shear and tilt moduli but a finite compressibility, (ii) a transverse Meissner effect as well as a resistance against shear deformation, (iii) sample-to-sample fluctuations of the longitudinal magnetic susceptibility, and (iv) an exponential decay of positional correlations in the direction perpendicular to the defects in $d = 3$.

Since point disorder may formally become relevant below $d = 4$, we consider the stability of the planar glass with respect to weak point impurities. We find that the pinning energy due to point impurities in $d = 3$ behaves as

$$\overline{\langle \mathcal{H}_P \rangle} = \rho_0 \sum_{n \neq 0} \int d\mathbf{r} V_P(\mathbf{r}) e^{inG_D x} e^{-(nG_D)^2 \overline{\langle u^2 \rangle}/2}$$

$$\sim \rho_0 \sqrt{n_{imp} v_p^2 L_y L_z L_x} \, e^{-L_x/(2\xi_c)}, \quad (63)$$

and from this we conclude that weak point impurities are an irrelevant perturbation. Similarly, it can be shown that pinning energy of randomly distributed *columnar* defects decays exponentially with L_x and hence does not destroy the planar glass.

D. Stability of the Bragg glass and the weakly pinned Bose glass

In this subsection we continue discussion of the competition between pinning effects due to point impurities and columnar and planar defects. We shall show that the weakly pinned Bose glass is stable with respect to weak point impurities but unstable with respect to weak planar defects. Moreover, we shall demonstrate that the Bragg glass phase is unstable with respect to both weak planar and weak columnar defects. The resulting phase diagram is shown schematically in Fig. 1.

First we discuss the stability of the Bragg glass phase in analogy to the test for stability of the planar glass in the previous subsection. We note that the correlation functions in the Bragg glass phase can also be obtained from a model with a uniaxial displacement field of FLs.[7] A uniaxial displacement field describes also properly charge-density

waves, a stack of membranes under tension, and domain walls in magnets. Justified by these observations, we first consider a uniaxial displacement field in the direction perpendicular to the defect planes. At the Bragg glass fixed point in $d=3$ the pinning energy of the planar defects behaves as

$$\overline{\langle \mathcal{H}_D \rangle} = \rho_0 \sum_{n \neq 0} \int d\mathbf{r} V_D(\mathbf{r}) e^{inG_D x} e^{-(nG_D)^2 \overline{\langle u^2 \rangle}/2}$$

$$\sim \rho_0 \sqrt{v^2 L^5 / \ell_D} L^{-\pi^2/18}. \tag{64}$$

When we compare this energy to the pining energy of point impurities,

$$\overline{\langle \mathcal{H}_P \rangle} \sim \sqrt{L^3 R_P^*(0)} \sim L, \tag{65}$$

we find that planar defects are a relevant perturbation. Note that at the Bragg glass fixed point the system is isotropic, i.e., $L_x = L_y = L_z = L$. In Eq. (65) we used the fact that the fixed-point correlator on the length scale L behaves as $R_P^*(0) \sim L^{-1}$ [cf. Eq. (18)]. Similarly, the pinning energy of columnar defects at the Bragg glass fixed point scales as

$$\overline{\langle \mathcal{H}_C \rangle} \sim \rho_0 \sqrt{v_c^2 n_{cd} L^4} L^{-\pi^2/18}, \tag{66}$$

and drives the system away from the Bragg glass fixed point. v_c and n_{cd} denote the strength and the density of columnar defects, respectively.

A functional RG analysis of weak columnar defects in $d = 5 - \epsilon$ yields a stable phase with a zero-temperature fixed point that is characterized by a power-law decay of the positional correlation function with an exponent $\eta_C = (\pi/3)^2(5 - d)$ and a transverse Meissner effect.[51] One can expect that this phase, found for an uniaxial displacement field, applies to the case where the FL density is larger than the columnar defect density, corresponding to the so-called weakly pinned Bose glass. In order to study the stability of this phase in $d = 3$ with respect to planar defects and point impurities, we compare the scaling

$$\overline{\langle \mathcal{H}_D \rangle} \sim \rho_0 \sqrt{v^2 L^3 L_z^2 / \ell_D} L^{-(\pi/3)^2}, \tag{67}$$

$$\overline{\langle \mathcal{H}_C \rangle} \sim \sqrt{R_c^*(0) L^2 L_z^2} \sim L_z, \tag{68}$$

$$\overline{\langle \mathcal{H}_P \rangle} \sim \rho_0 \sqrt{v_p^2 n_{imp} L^2 L_z} L^{-(\pi/3)^2} \tag{69}$$

of the different pinning energies, where we used $L_x = L_y = L$ and columnar disorder fixed-point correlator $R_C^*(0) \sim L^{-2}$. We conclude that weak point impurities are irrelevant but weak planar defects are relevant in the weakly pinned Bose glass.

Next we examine the stability of the Bragg glass phase by considering a vector displacement field. This displacement field reveals the triangular lattice structure of the FLL. By changing the orientation of the defect planes, the number of FLs that are pinned by the defects changes. In $d = 3$ we have

$$\overline{\langle \mathcal{H}_D \rangle} \sim \rho_0 \sqrt{v^2 L^5 / \ell_D} e^{-G_D^2 \overline{\langle u_x^2 \rangle}/2} \sim L^{5/2 - g}, \tag{70}$$

$$\overline{\langle \mathcal{H}_C \rangle} \sim \rho_0 \sqrt{v_c^2 n_{cd} L^4} e^{-\overline{\langle (\mathbf{G}_0 \mathbf{u})^2 \rangle}/2} \sim L^{2 - \eta/2}, \tag{71}$$

$$\overline{\langle \mathcal{H}_P \rangle} \sim \sqrt{L^3 R_P^*(0)} \sim L, \tag{72}$$

where g is given by Eq. (25), $|\mathbf{G}_0| = 4\pi/(\sqrt{3}a)$ is the shortest vector of the reciprocal lattice and η is the exponent of the positional correlation function in the Bragg glass phase. Weak columnar defects are always a relevant perturbation, while weak planar defects are relevant only if they satisfy $g < g_c = 3/2$, i.e., only if they are parallel to the main crystallographic planes of the FLL. Here we neglected the influence of weak planar defects on the elasticity of the FLL. In fact, the defects lead to an additional anisotropy in the elastic energy which is associated with a larger energy for deformations with nonzero $\partial_y u_x$ and $\partial_z u_x$. Through a renormalization of the elastic constants g is renormalized downwards. Therefore, stronger planar defects lead to an increased $g_c > 3/2$, rendering additional orientations of defects relevant. However, it is likely that in the case of a finite density of parallel defect planes, the FLL will rotate to a position in which it reaches maximum overlap with the defects. Then the planar defects will be parallel to the main lattice planes and the Bragg glass is unstable.

V. FINITE DENSITY OF STRONG DEFECTS

In this section we consider the FLL with a finite density of parallel, randomly distributed defect planes that are aligned to the magnetic field. The defects are assumed to be sufficiently strong so that the Larkin length [see Eq. (54)] is of the order of the mean defect spacing or smaller, $L_D \lesssim \ell_D$. In this case the defect potential cannot be treated perturbatively with respect to the elastic energy, and a new approach is required. Here we derive an effective Hamiltonian that is defined only at the defect planes. We determine the ground-state configuration of the FLL and calculate the positional correlation function. We show that a transverse Meissner effect as well as a resistance against shear deformations appears also in this case.

The Hamiltonian in $d = 3$ dimensions reads

$$\mathcal{H} = \mathcal{H}_0 + \sum_i^{N_D} \mathcal{H}_{D,i}, \tag{73}$$

where $\mathcal{H}_0$ is the elastic Hamiltonian given by Eq. (2) and $\mathcal{H}_{D,i}$ is the pinning energy of the defect plane at the position $x = x_i$ [see Eq. (22)]. N_D denotes the number of defects. In this section we consider a simplified model involving only uniaxial displacements perpendicular to the defects $\mathbf{u} = u\hat{\mathbf{x}}$. In Sec. VII we shall discuss the implications of the generalization to a two-dimensional vector displacement. The part of $\mathcal{H}_D$ that describes the coupling of the pinning potential to the slowly varying part of the FL density ($\sim \partial_x u$) leads only to an increase in the FL density at the defects and can be eliminated by applying the transformation

$$u(\mathbf{r}) \rightarrow u(\mathbf{r}) - v\rho_0/c_{11} \sum_{i=1}^{N_D} \Theta(x - x_i), \tag{74}$$

where $\Theta(x) = 0$, $x \leq 0$ and $\Theta(x) = 1$, $x > 0$. The Hamiltonian then becomes

$$\mathcal{H} = \mathcal{H}_0 - 2v\rho_0 \sum_{i=1}^{N_D} \int_{y,z} \sum_{k>0}^{[\ell/\xi]_G} \cos\{kG_D[u(x,y,z) - \alpha_i]\}, \tag{75}$$

where $\alpha_i = x_i + v\rho_0(i-1)/c_{11}$. For simplicity we assume that all defects have the same strength.

In order to obtain a Hamiltonian that is isotropic in the yz plane, we introduce the rescaled coordinate $z' = z\sqrt{c_{66}/c_{44}}$ and define $u'(y,z') = u(y,z)$. We shall omit the primes below. We proceed by studying the ground state of the displacement field for a given distribution of planar defects, assuming that a strong defect potential suppresses thermal fluctuations. First we solve the saddle-point equation in the gap between the defects with prescribed, but arbitrary, boundary conditions at the defects $u_i(y,z) = u(x_i,y,z)$ with Fourier transform $\tilde{u}_i(\mathbf{q}) = \tilde{u}(x_i, \mathbf{q})$, $\mathbf{q} = (q_y, q_z)$. In the ground-state configuration the FLs are completely aligned to the defect planes and $u(x_i,y,z)$ is independent of y and z. However, we derive the saddle-point solution and the effective Hamiltonian for a more general displacement field configuration at the defect planes since this will be necessary for a discussion of the transverse Meissner effect below as well as the FL dynamics in Sec. VI. In the following we use the notation $\Delta A_i = A_{i+1} - A_i$ for any quantity A. The solution of the saddle-point equation between two defect planes reads, with $x \in [x_i, x_{i+1}]$,

$$\tilde{u}(x, \mathbf{q}) = \frac{\tilde{u}_i(\mathbf{q})}{\sinh(q'\Delta x_i)} \sinh[q'(x_{i+1} - x)] + \frac{\tilde{u}_{i+1}(\mathbf{q})}{\sinh(q'\Delta x_i)} \sinh[q'(x - x_i)], \tag{76}$$

where $q' = \sqrt{c_{66}/c_{11}}q$. Note that we have solved the saddle-point equation between the defects within a continuum model and not on the lattice. This amounts to setting the momentum cutoff $\Lambda \to \infty$. After substituting this solution into the Hamiltonian of Eq. (75) and integrating over x, the Hamiltonian reduces to

$$\mathcal{H} = \frac{\sqrt{c_{11}c_{44}}}{2} \int \frac{d^2q}{(2\pi)^2} q \sum_{i=1}^{N_D-1} \left\{ \frac{|\tilde{u}_{i+1}(\mathbf{q}) - \tilde{u}_i(\mathbf{q})|^2}{\sinh\left(q\Delta x_i \sqrt{\frac{c_{66}}{c_{11}}}\right)} + (|\tilde{u}_i(\mathbf{q})|^2 \right.$$
$$\left. + |\tilde{u}_{i+1}(\mathbf{q})|^2) \tanh\left(\frac{q\Delta x_i}{2} \sqrt{\frac{c_{66}}{c_{11}}}\right) \right\}$$
$$- 2v\rho_0 \sqrt{\frac{c_{44}}{c_{66}}} \sum_{i=1}^{N_D} \int_{y,z} \sum_{k>0}^{[\ell/\xi]_G} \cos\{kG_D[u_i(y,z) - \alpha_i]\}. \tag{77}$$

A similar Hamiltonian has been obtained for a Luttinger liquid with point impurities.[57]

Next we study the ground state of the FLL. In the limit $v \to \infty$ the FLs are completely aligned to the defects and $u_i(y,z) = u_i$. Then the Hamiltonian of Eq. (77) becomes

$$\frac{\mathcal{H}}{L^2}\sqrt{\frac{c_{66}}{c_{44}}} = \frac{c_{11}}{2} \sum_{i=1}^{N_D-1} \frac{(u_{i+1} - u_i)^2}{\Delta x_i}$$
$$- 2v\rho_0 \sum_{i=1}^{N_D} \sum_{k>0}^{[\ell/\xi]_G} \cos\left[k\frac{2\pi}{\ell}(u_i - \alpha_i)\right], \tag{78}$$

where L is the system size. For $u_i = \ell n_i + \alpha_i$, where n_i is an integer number, the energy gain of the FLs from the defect potential is maximal. We determine n_i such that the elastic energy is minimal and find the ground-state configuration to be degenerate and given by[58]

$$u_i^{(n)} = \ell\left(\frac{\alpha_i}{\ell} - \sum_{j<i}\left[\frac{\Delta\alpha_j}{\ell}\right]_G + n\right), \tag{79}$$

where n is an integer number. Note that this is the ground-state configuration for an arbitrary defect strength in the special case when $\Delta\alpha_i/\ell - [\Delta\alpha_i/\ell]_G = 0$ for all i. Then the FLs are just shifted in order to gain energy from the defects without any elastic energy loss. However, for randomly distributed defect planes that satisfy $\ell_D \gg \ell$, $\Delta\alpha_i/\ell - [\Delta\alpha_i/\ell]_G$ is uniformly distributed in the interval $[-1/2, 1/2]$. Using the central limit theorem, we find that the positional correlation function decays exponentially fast in the x direction,

$$S_{\mathbf{G}_D}(\mathbf{r}) \sim e^{-|x|/\xi_c}, \quad x \gg \ell_D \tag{80}$$

with $\xi_c \approx 6\ell_D/\pi^2$. This shows that the limits of weak and strong planar defects lead to the same behavior of the positional correlations in $d=3$. The correlation length in both cases is determined by the Larkin length of the defects.

From the shifted boundary conditions $u_i(y, z \to \infty) = u_i^0 + \ell$ and $u_i(y, 0) = u_i^0$ one can obtain also the interface tension Σ_z and it turns out to be finite. We do not quote the result here since it is cutoff dependent and hence nonuniversal. Also, a general expression that is valid for all ratios of the elastic constants is not available. A similar analysis shows that the surface tension Σ_y is finite. Hence, strong defects lead to a transverse Meissner effect as well as a resistance against shear deformations. The finite values of Σ_z and Σ_y might be interesting to probe experimentally.

VI. FLUX-LINE CREEP

The technologically the most interesting property of type-II superconductors is their ability to carry a bulk current with as little dissipation as possible. The Lorentz force acts on FLs and hence gives rise to dissipation.[1] Pining centers play an important role in preventing FL motion and lead to a nonlinear resistivity $\ln \rho \sim -J^{-\mu}$ for $J \to 0$, which depends on the so-called creep exponent μ.[3,54] In this section we study the effect of planar defects on the FL dynamics in the direction perpendicular to the defect planes. The defects are assumed to be parallel to the applied magnetic field. For a single defect plane we show that the creep exponent is $\mu = 1$, apart from logarithmic corrections. We find that many planar defects act as a more effective source of pinning than point impurities[4] and columnar defects.[3,11,12] They considerably slow down the FLs in comparison to the Bragg glass

and the Bose glass, leading to a creep exponent $\mu = 3/2$ for the planar glass.

A. Single defect

First we discuss the creep of FLs in the presence of a single planar defect, aligned to the applied magnetic field and without point impurities, for currents parallel to the defect and perpendicular to the magnetic field. The Hamiltonian is given by $\mathcal{H} = \mathcal{H}_0 + \mathcal{H}_D + \mathcal{H}_{\text{force}}$, where the part describing elastic deformations, $\mathcal{H}_0$, is given by Eq. (2), the defect pinning energy $\mathcal{H}_D$ by Eq. (22) and the Lorentz force contribution reads

$$\mathcal{H}_{\text{force}} = -\int d^3\mathbf{r} \{\mathbf{J}(\mathbf{r}) \times \mathbf{B}(\mathbf{r})\} \cdot \mathbf{u}(\mathbf{r}). \tag{81}$$

$\mathbf{J}(\mathbf{r})$ is the current density, $\mathbf{B}(\mathbf{r})$ is the magnetic induction and the speed of light is set to one. Since we will consider only FL dynamics normal to the defect and since the defect potential depends only on the perpendicular displacement field, it appears plausible to simplify our model and to consider a uniaxial displacement field in the direction perpendicular to the defect plane.

The defect plane is a relevant perturbation in the Shubnikov (mixed) phase for all orientations of the plane (in contrast to the case when point impurities are present) since thermal fluctuations do not roughen the FLL in $d = 3$. This can be easily seen from the RG Eq. (28) by setting $g = 0$. Under renormalization the weak defect potential that couples to the periodic part of the FL density grows and flows to strong coupling. Since we are interested in the small current densities $J \to 0$ which probe large length scales, we shall study only the strong defect plane below. Our results apply also to weak defects at sufficiently large length scales or small currents.

In the absence of a current, the FLs are aligned to the defect plane and the ground state is highly degenerate. Different ground states differ by a shift of the displacement field by ℓ because the energy does not depend on which FLL plane is pinned by the defect. This degeneracy is broken when a current is turned on and the original ground state becomes unstable. The system now evolves into a new metastable state that is lower in energy and in which the FLs are shifted by ℓ. This process is enabled via the formation of droplets which are nuclei of new metastable states. The competition between bulk energy gain and elastic energy loss determines the energy (and size) of the critical droplet. The energy of the critical droplet corresponds to the energy barrier that the FLs have to overcome when evolving to a new state. Thermally activated FL hopping over barriers with energy $E_{\text{drop}}^*(J)$ determines the resistivity through the Arrhenius law[59,60]

$$\rho(J) \sim e^{-E_{\text{drop}}^*(J)/T}. \tag{82}$$

Therefore, we need to estimate $E_{\text{drop}}^*(J)$.

We proceed by deriving an effective Hamiltonian that is defined on the defect plane ($x = 0$). By integrating out the displacement field off the defect we get (see Appendix B)
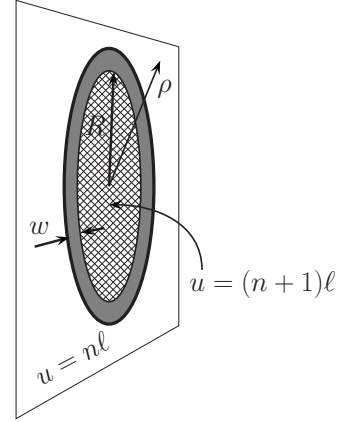

FIG. 4. Schematic illustration of a droplet with radius R and width w at a defect plane.

$$\begin{aligned}
\mathcal{H}_{eff} = \frac{1}{2}\int \frac{d^2\mathbf{q}}{(2\pi)^2} |\tilde{u}(0, q_y, q_z)|^2 [\tilde{\mathcal{G}}(0, \mathbf{q})]^{-1} \\
- 2v\rho_0 \int dy\, dz \sum_{k > 0}^{[\ell/\xi]_G} \cos[kG_D u(0, y, z)] \\
- \tilde{u}(0, \mathbf{q} = 0) \int dx\, J(x) B(x).
\end{aligned} \tag{83}$$

Here $\mathbf{q} = (q_y, q_z)$ is the in-plane momentum, $\tilde{u}(0, q_y, q_z) = \tilde{u}(x = 0, q_y, q_z)$ and

$$\tilde{\mathcal{G}}(0, \mathbf{q}') = \frac{\arctan\left[\dfrac{\Lambda}{|\mathbf{q}'|}\sqrt{\dfrac{c_{11}}{c_{66}}}\right]}{\pi|\mathbf{q}'|\sqrt{c_{11}c_{66}}}, \tag{84}$$

where $\mathbf{q}' = (q_y, \sqrt{c_{44}/c_{66}}q_z)$ and $\Lambda = 2\pi/\lambda$. Since the system is translationally invariant in the yz plane, the current density and magnetic induction depend only on x. In order to simplify the computations, we make the system isotropic in the yz plane by the rescaling $z' = z(c_{66}/c_{44})^{1/2}$ and $u'(\mathbf{r}') = u(\mathbf{r})$. In the following we will omit the primes.

The critical droplet is a solution of the saddle-point equation for the Hamiltonian of Eq. (83) with fixed boundary conditions $u(0, \rho \to 0) = (n+1)\ell$ and $u(0, \rho \to \infty) = n\ell$ with $\rho = (y^2 + z^2)^{1/2}$ and n integer. For the precise solution see, e.g., a related discussion for a single strong impurity in a Luttinger liquid in Ref. 61. The shape of the droplet is characterized by its radius R and the width w of the droplet wall (see Fig. 4) so that the displacement field obeys approximately

$$u(0, \rho) \approx \begin{cases} (n+1)\ell, & \rho \in [0, R] \\ n\ell, & \rho \in [R + w, \infty]. \end{cases} \tag{85}$$

The exact shape of the droplet wall is not essential for the discussion that follows. We assume that it smoothly interpolates between $(n+1)\ell$ and $n\ell$. The width w of the droplet wall does not depend on the radius for small currents $J \to 0$. In this limit the critical droplet radius is much larger than the width $R \gg w$ so that the energy loss is balanced by the energy gain from the Lorentz force (see, e.g., Ref. 62 and references

therein). The critical droplet radius and energy is determined by maximizing the droplet energy $E_{\text{drop}}(R)$.

Since across the droplet wall the FLs are not aligned to the defect plane, a strong defect tends to reduce the width of the wall. Then, the large-$\mathbf{q}$ behavior of the propagator of Eq. (84), $[\tilde{\mathcal{G}}(0,\mathbf{q})]^{-1} \approx (\pi c_{66} q^2)/\Lambda$, becomes important at the wall since it describes elastic deformations on small length scales. For sufficiently strong defects ($w \simeq \Lambda^{-1}$) the precise form of the droplet wall is determined by the interplay between the elastic energy $\sim q^2$ and the defect pinning energy. The energy loss for FLs at the defect plane is[61] $E_{\text{core}} \sim Rv^{1/2}$, as known from droplets in the sine-Gordon model.

The elastic energy loss outside the plane, due to the deformation of the FLs at the defect plane is determined by the low-$\mathbf{q}$ behavior of the propagator of Eq. (84), $[\tilde{\mathcal{G}}(0,\mathbf{q})]^{-1} \approx 2\sqrt{c_{11}c_{66}}|\mathbf{q}|$, since the deformation occurs across the large scale R. It captures the three-dimensional nature of the FLL by its nonlocal form $\sim|\mathbf{q}|$. This is obvious when the elastic energy is written as

$$\mathcal{H}_{el} = \frac{\sqrt{c_{11}c_{44}}}{4\pi} \int d^2\mathbf{r}_1 \int d^2\mathbf{r}_2 \frac{[u(\mathbf{r}_1) - u(\mathbf{r}_2)]^2}{(\mathbf{r}_1 - \mathbf{r}_2)^3}. \quad (86)$$

Here $\mathbf{r}_1$ and $\mathbf{r}_2$ lay in the defect plane and satisfy $|\mathbf{r}_1 - \mathbf{r}_2| > \lambda$. The long-ranged elasticity in the effective two-dimensional elastic Hamiltonian of Eq. (86) results from fluctuations outside the defect plane that have been integrated out. Since $R \gg w$, the precise form of the droplet wall is not important for estimating $\mathcal{H}_{el}$ and we can assume $w = 0$ (corresponding to $v \to \infty$). Then we obtain for the elastic energy

$$E_{el} \approx 2\sqrt{c_{11}c_{44}}\ell^2 R \log(R/\lambda). \quad (87)$$

This result can be interpreted as the energy of charges of equal sign (corresponding to kinks in the displacement field) which are placed along a circle of radius R and interact via the three-dimensional Coulomb potential.

The energy losses mentioned above are balanced by an energy gain due to the Lorentz force that is described by the last term of Eq. (83),

$$E_{\text{force}} \approx \ell R^2 \pi \sqrt{\frac{c_{44}}{c_{66}}} \int dx J(x) B(x). \quad (88)$$

When we estimate E_{force}, a finite width of the droplet wall can be neglected since $R \gg w$. The total droplet energy then reads

$$E_{\text{drop}} \approx E_{el} + E_{\text{core}} - E_{\text{force}} \approx \alpha R \log\left(\frac{R}{\lambda}\right) + R\beta - \gamma R^2, \quad (89)$$

where $\alpha = 2(c_{11}c_{44})^{1/2}\ell^2$, $\beta \sim v^{1/2}$ and $\gamma = \pi(c_{44}/c_{66})^{1/2}\ell \int dx J(x) B(x)$. The creep rate is determined by the droplet with the largest total energy E_{drop}, which is called the critical droplet. Solving the equations $\partial_R E_{\text{drop}} = 0$ and $\partial_R^2 E_{\text{drop}} < 0$ we find the size R^* and the energy E_{drop}^* of the critical droplet. Increasing of the droplet radius beyond R^* does not cost any energy and droplet freely expands. For $R \to \infty$ the system reaches a new metastable state in which all

FLs are shifted by ℓ perpendicular to the defect. The nonlinear resistivity is given by the Arrhenius law. In the limit of a vanishing current density, i.e., for large β/γ, we get

$$\rho \sim e^{-E_{\text{drop}}^*/T} \sim \exp\left\{ -\frac{1}{4\gamma T}\left[\left(\beta + \alpha \log\frac{\beta + \alpha}{2\lambda\gamma}\right)^2 - \alpha^2 \right] \right\}. \quad (90)$$

Prefactors are not determined here since in the limit of a vanishing current density the current-voltage characteristic is dominated by the exponential factor of Eq. (90). The result for ρ yields the creep exponent $\mu = 1$ plus logarithmic corrections. To estimate the coefficient γ we need to know how the current density and the magnetic induction vary in space. This is a tedious analysis which goes beyond the scope of the present study and is left for further investigation.

Next we examine how randomly distributed weak point impurities around the defect plane affect the FL creep for $J \to 0$. A weak defect is relevant in the RG sense only for $g < 1$ and it then flows to the strong-coupling limit. Criteria for the relevance of a strong defect with an arbitrary orientation are not available. Therefore we study below only the strong-coupling limit for a defect that is oriented parallel to the main FLL planes. We expect that the liberation from the defect plane is the limiting factor for the FL motion so that the creep exponent is reduced compared to its value in the BG phase.

The shape of the droplet is again given by Eq. (85) but now the impurities control the fluctuations of the FLs outside the defect. Without point impurities, the displacement field decays outside the defect plane as $u(x, \rho=0) \approx (\ell/2)(R/x)^2$ for $x \gg R$. Pointlike impurities induce additional displacement fluctuations and the droplet-induced deformations are no longer long-ranged. This can be seen from the correlation function in the presence of a relevant defect that follows from Eq. (40),

$$\langle [u(x,\rho) - u(0,\rho)]^2 \rangle = \frac{1}{2}\langle [u(x,\rho) - u(-x,\rho)]^2 \rangle_{BG}. \quad (91)$$

The subscript BG means that the correlation function is computed at the BG fixed point. Since the right-hand side of Eq. (91) is of the order a^2 for $x \approx L_a$ we conclude that the droplet extends up to L_a from the defect. This yields for the energy gain from the Lorentz force the rough estimate $E_{\text{force}} \approx JBL_aR^2\ell$ where J is the mean current density inside the droplet. Hence, in the limit $J \to 0$ resistivity is

$$\rho(J) \sim \exp\left[-\frac{C_1}{J}\left(\log\frac{C_2}{J}\right)^2 \right], \quad (92)$$

where C_1 and C_2 depend on T, B, the strength and concentration of the impurities and on the defect strength. This result shows that a single relevant defect plane indeed slows down the FL creep in comparison to the BG phase.

B. Finite density of weak defects

Here we consider FL creep perpendicular to many weak defects with random positions but in the absence of point impurities, cf. Sec. IV. The motion of FL bundles under the
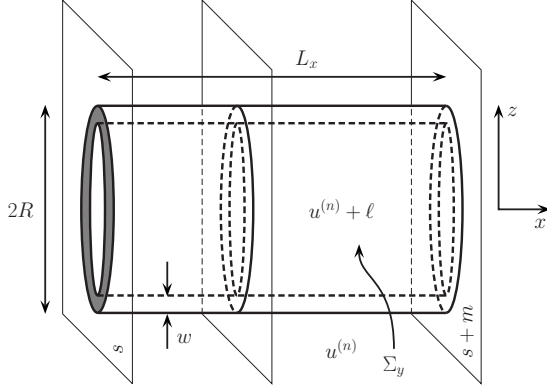
FIG. 5. Schematic representation of a cylindrically shaped droplet of radius R and length L_x that extends across more than one defect plane. It drives the system into the new metastable state $u^{(n)} + \ell$. Note that domain walls parallel to the defects are wide (not shown here), while the cylindrically shaped domain wall is narrow (of width w).

influence of the Lorentz force is again driven by the nucleation of critical droplets.[3] A typical droplet is schematically shown in Fig. 5. For small currents, the droplet extends over many defect planes in order to balance elastic and pinning energy loss with bulk energy gain from the Lorentz force. For small current densities, the FLL is properly described in terms of the interface tensions Σ_y and Σ_z, see Eq. (51), which are appropriate on sufficiently large length scales. The energy of the droplet is then of the form

$$E_{\text{drop}} \approx \sqrt{\frac{c_{44}}{c_{66}}} L_x^{d-2} R^2 \left(\frac{c_{11}\ell^2}{L_x^2} + \frac{\Sigma_y}{R} - JB\ell \right). \quad (93)$$

The elastic energy cost for the formation of the droplet consists of two terms. The first term of Eq. (93) is the energy of a wide domain wall of width $\sim L_x$ parallel to yz plane. The second term of Eq. (93) describes the energy of a narrow cylindrically shaped domain wall perpendicular to yz plane. In the estimate of E_{drop} we have taken into account that the elastic energy and the energy from planar disorder scale in the same way. The last term of Eq. (93) is the energy gain from the Lorentz force. $J(B)$ is to be understood as the mean current density (magnetic induction) averaged over the defect spacing.

Note that we have used again the rescaling $z' = (c_{66}/c_{44})^{1/2}z$. In Eq. (93) we have taken into account the logarithmic roughness of the displacement field, corresponding to the roughness exponent $\zeta = 0$. We have ignored logarithmic corrections. The σ term of Eq. (45), that is responsible for the roughness exponent $\zeta = 1/2$, can be eliminated by the simple transformation that was discussed in Sec. IV and hence it does not affect the FL dynamics. In case of a potential breakdown of the ϵ expansion (cf. Sec. IV B) in $d = 3$ and the existence of a strong-coupling fixed point,[55] see Sec. VI C.

To determine the critical droplet we solve $\partial_{L_x} E_{\text{drop}} = 0$ and $\partial_R E_{\text{drop}} = 0$. We find for the critical radius R^* and the critical length L_x^* of the droplet

$$\frac{R^*}{\Sigma_y} \sim \frac{L_x^{*2}}{c_{11}\ell^2} \sim \frac{1}{JB\ell}. \quad (94)$$

This yields for $d = 3$ the nonlinear resistivity in the limit $J \ll J_D$,

$$\rho(J) \sim e^{-(J_D/J)^{3/2}}, \quad J_D = \mathcal{C}\frac{(\Sigma_y\Sigma_z)^{2/3}(c_{11}/\ell)^{1/3}}{BT^{2/3}}. \quad (95)$$

Here $\mathcal{C}$ is positive numerical constant of order unity. Thus the nonlinear resistivity is considerably reduced compared to the Bragg glass phase and to a single defect plane in the presence of impurities.

In the similar way one can consider the creep in the presence of randomly distributed columnar defects that are aligned to the applied magnetic field and have a mean spacing that is larger than FL spacing. Based on a functional RG in $d = 5 - \epsilon$ dimensions,[51] we obtain the creep exponent $\mu = 1$. This result is in agreement with the one derived in Ref. 3 by other means. The result is expected to apply to the weakly pinned Bose glass phase.

C. Finite density of strong defects

Here we discuss the analog of the previous subsection in the limit of strong defects, see Sec. V. The ground-state degeneracy given by Eq. (79) is broken when a current is applied. The system evolves between different ground states via the formation of critical droplets. For small currents $J \ll c_{11}\ell/(B\ell_D^2)$ the critical droplet extends over many defect planes and we obtain the creep exponent $\mu = 3/2$. For moderate currents with $c_{11}\ell/(B\ell_D^2) \ll J \ll v/(\phi_0\xi\ell_D)$ the droplet forms only at a single defect plane and we recover Eq. (90) with $\gamma \approx (c_{44}/c_{66})^{1/2}\ell\ell_D JB$, i.e., a creep exponent $\mu = 1$.

We assume that the saddle-point solution for u_i with fixed boundary conditions $u_i(\rho \to 0) = u_i^{(n+1)}$ and $u_i(\rho \to \infty) = u_i^{(n)}$ obeys Eq. (85). At each defect plane, the radius R_i and the center of the droplet can be different. However, it is plausible to assume that in the saddle-point configuration the droplet is centered at the same lateral position in each plane and all droplets have the same radius R since the droplet tends to maximize its volume while keeping the surface minimal. Specifically, we assume that the droplet is located between the sth and the $(s+m)$th defect plane.

The width of the droplet wall for a sufficiently strong defect potential satisfies $w \ll \ell_D$ and $w \ll R$. The precise form of the wall is not important in finding the energy of a domain wall parallel to the defects as well as the bulk energy gain. Hence, we set the width of the droplet to zero which yields for the Fourier transform of the displacement at the ith defect plane,

$$\tilde{u}_i(\mathbf{q}) = 2\pi R\ell \frac{J_1(qR)}{q} + u_i^{(n)}(2\pi)^2\delta(\mathbf{q}), \quad (96)$$

where J_1 is the Bessel function of the first kind. Due to the transport current we have to add to the Hamiltonian of Eq. (77) the additional energy

$$H_{\text{force}} = -\sum_{i=1}^{N_D-1} \int_{x_i}^{x_{i+1}} dx f(x) \left\{ \frac{\tilde{u}_i(0)}{\Delta x_i}(x_{i+1}-x) \right.$$
$$\left. + \frac{\tilde{u}_{i+1}(0)}{\Delta x_i}(x-x_i) \right\}, \tag{97}$$

where $f(x)=(c_{44}/c_{66})^{1/2}J(x)B(x)$. By substituting the Eq. (96) into Eq. (77), we find that the droplet energy has a different form for $R \gg \ell_D\sqrt{c_{66}/c_{11}}$ and $R \ll \ell_D\sqrt{c_{66}/c_{11}}$.

First we discuss the case $R \gg \ell_D\sqrt{c_{66}/c_{11}}$. The droplet energy reads then

$$E_{\text{drop}} = \Sigma_x R^2 \pi + \Sigma_y 2R\pi m\ell_D - JB\ell R^2\pi m\ell_D\sqrt{\frac{c_{44}}{c_{66}}}. \tag{98}$$

In order to explain and interpret the first term of Eq. (98), we consider an excited state with

$$u_i^{\pm} = \begin{cases} u_i^{(n)} & \text{for} \quad i \le k \\ u_i^{(n\pm1)} & \text{for} \quad i > k. \end{cases} \tag{99}$$

This state describes a domain wall parallel to the defects. Using Eq. (78), it can be shown that for a given disorder realization the energy cost of such wall per unit surface area is

$$\Sigma_x^{\pm}(k) = c_{11}\sqrt{\frac{c_{44}}{c_{66}}}\frac{\ell^2}{2\Delta x_k}\left[1 \pm 2\left(\frac{\Delta\alpha_k}{\ell} - \left[\frac{\Delta\alpha_k}{\ell}\right]_G\right)\right]. \tag{100}$$

Since the droplet consists of two such walls (see Fig. 5), the surface tension in the first term of Eq. (98) is given by

$$\Sigma_x = \Sigma_x^+(s-1) + \Sigma_x^-(s+m). \tag{101}$$

The droplet takes advantage of fluctuations in the surface tension Σ_x and the lowest value of Σ_x for a droplet of length $L_x=m\ell_D$ is typically of the order $c_{11}\sqrt{c_{44}/c_{66}}\ell^2/L_x$ when $\ell_D \gg \ell$. We point out that this result is in agreement with the statistical tilt symmetry.

The second term of Eq. (98) is the energy cost for the domain wall perpendicular to the defects with surface tension Σ_y. We do not provide here an explicit expression for Σ_y, for the reasons discussed in Sec. V. Note that Σ_y carries information about the strength and density of defect planes. By ignoring the spatial variations of J and B, we get the average bulk energy gain to be given by the last term in Eq. (98).

By solving $\partial_m E_{\text{drop}}=0$ and $\partial_R E_{\text{drop}}=0$ we determine the radius R^* and length $L_x^*=m^*\ell_D$ of the critical droplet. With this parameters, Eq. (98) yields the energy of the critical droplet. We find that this energy leads, up to unimportant prefactors, to the same nonlinear resistivity as in the weak pinning case of Eq. (95). This result is valid for sufficiently small currents such that $R^* \gg \ell_D\sqrt{c_{66}/c_{11}}$ and $m^* \gg 1$. The latter condition results from treating m as a continuous variable which is a reasonable approximation for critical droplet that extends across a large number of defect planes. These conditions translate to the requirement $J \ll c_{11}\ell/(B\ell_D^2)$ for the current density.

Next, we shortly discuss the droplet expansion when it reaches the radius R^* and the length L_x^*. By analyzing the Hessian matrix of E_{drop} we find that the eigenvector that points into the direction of the free droplet expansion has a x component that is much smaller than its ρ-component, i.e., an expansion of the cross section of the cylinder is favorable over an expansion of its length. In order to describe a potential growth in the x direction, one has to know the set of numbers $\Sigma_x(i)^{\pm}$ that depends on the disorder realization. However, the droplet will get stuck between planes with low Σ_x and a further expansion along the x axis costs energy.

Droplets occur and expand independently across the entire sample. After the FLs have moved in some regions, the boundaries of these regions will be favorable sites for emergence of new droplets.[62] Indeed, after the formation and expansion of a droplet up to the $(i-1)$th defect plane such that $u_k=u_k^{(n+1)}$ for $k \le i-1$ and $u_k=u_k^{(n)}$ for $k \ge i$, the new surface tension reads

$$\Sigma_x'^+(i-1) = -\Sigma_x^-(i-1) < 0. \tag{102}$$

The reason for this result is that after the droplet expansion an additional FLL plane appears with respect to the initial ground state between ith and $(i-1)$th planes and the FLs are compressed. The formation of a new droplet at the ith plane is favorable because it allows the system to relax into the new ground-state configuration between $(i-1)$th and ith plane. Since the droplet described by Eq. (98) has the longest life time, the resistivity is determined by $\rho \sim \exp(-E_{\text{drop}}^*/T)$, where the critical energy E_{drop}^* is given by Eq. (98) evaluated at R^* and L_x^*.

When comparing Eq. (95) with the creep exponent $\mu =1/2$ of the defect-free BG phase, we see that defect planes act as a more efficient source of pinning in stabilizing superconductivity than point impurities. However, we have considered only typical droplets in estimating Σ_x. For system sizes $L \gg \ell_D$ it is likely that rare regions with untypically large Σ_x will appear and in turn determine the resistivity. We leave this problem for further investigations.

Next, we consider the case $R \ll \ell_D\sqrt{c_{66}/c_{11}}$. From the second term of Eq. (77) we find that for m defect planes the energy loss given by Eq. (87). The first term in Eq. (77), which describes the coupling between neighboring defects, provides a much smaller contribution than the second term and can be neglected. Then the defects are effectively decoupled, and the nucleus energy is

$$E_{\text{drop}} = mE_{\text{single}}. \tag{103}$$

Here E_{single} is the energy of the droplet that appears in the case of a single defect plane. It is given by Eq. (89) with the system size replaced by the mean defect distance ℓ_D. The nucleus energy grows with increasing m so that it is minimal for $m=1$ and the critical droplet is located at one defect plane only. Nonlinear resistivity is then again given by Eq. (90), but with $\gamma \approx (c_{44}/c_{66})^{1/2}\ell\ell_D JB$. This result is valid for intermediate currents $c_{11}\ell/(B\ell_D^2) \ll J \ll v/(\phi_0\xi\ell_D)$.

VII. DISCUSSION

For a finite density of randomly distributed parallel planar defects with the magnetic field aligned to them, and with a

mean defect spacing that is larger than FL spacing, we find a phase of FLs at low temperatures, the planar glass. We considered mainly a simplified model with an uniaxial displacement field (which is also applicable to a wide class of other systems). Here we comment on possible consequences of this simplification by taking into account also the displacement field u_y parallel to the defects. The part of the defect Hamiltonian that describes the coupling of the defect potential to the slowly varying part of FL density can be eliminated by transforming u_x as described by Eq. (74). For strong planar defects each defect plane is occupied by a single FL layer and hence $u_x^{(n_i)}(x_i, y, z) = \ell n_i + \alpha_i$ for all y, z in order to maximize the pinning energy gain. Even in the absence of point disorder the displacement u_y does not vanish. This can be seen most easily in the case of isotropic elasticity where the following relations hold:

$$\sigma \partial_x u_x = -\partial_y u_y, \quad \sigma = \frac{c_{11} - c_{66}}{c_{11} + c_{66}}. \quad (104)$$

Here σ is the Poisson number with $-1 < \sigma < 1$.[36] The strain $\partial_x u_x$ in the gap between the defects at x_{i+1} and x_i is

$$\partial_x u_x \approx 1 + \frac{v\rho_0}{c_{11}\Delta x_i} + \ell \frac{\Delta n_i}{\Delta x_i}, \quad (105)$$

where we used the notation $\Delta A_i = A_{i+1} - A_i$ for a variable A. The difference of the strain $\partial_y u_y$ in neighboring gaps is then

$$\Delta \partial_y u_y \approx -\sigma \ell \left[\frac{\Delta n_{i+1}}{\Delta x_{i+1}} - \frac{\Delta n_i}{\Delta x_i} + \frac{v\rho_0}{c_{11}\ell}\left(\frac{1}{\Delta x_{i+1}} - \frac{1}{\Delta x_i} \right) \right], \quad (106)$$

which is of the order $\pm \sigma \ell / \ell_D$. On the scale L_y this implies $\Delta u_y \sim \pm \sigma \ell L_y / \ell_D$. To avoid a diverging shear energy, dislocations with a Burgers vector parallel to the y direction occur at the defect planes (see Fig. 6). Their distance along the y direction is of the order ℓ_D / σ. The energy of a pair of edge dislocations with antiparallel Burgers vectors at a distance ℓ_D is[63]

$$E_{\text{edge}} \approx \frac{c_{66}}{2\pi} a^2 L_z \ln\left(\frac{\ell_D}{a} \right). \quad (107)$$

This energy has to be compared with the energy gain from the defects which is of the order

$$E_D \approx -\frac{\ell}{\sigma\xi} L_z v \ell_D \rho_0. \quad (108)$$

Hence for $\sigma c_{66} a^3 \xi \ll \ell_D v$ the energy of the dislocations is overcompensated by the defect planes and dislocations will be present.

In general, the network of additional FLL sheets spanned by the dislocations will be complicated. The network follows from the solution of the equations of two-dimensional elasticity with the boundary condition $u_x(x_i, y, z) \equiv u_x^{(n_i)}(x_i, y, z)$ and the dislocation density $b_y(x_i, y)$ at each defect. The energy has to be minimized first with respect to $b_y(x_i, y)$ and the with respect to n_i.[64] The resulting state is completely ordered along the z direction. It is also ordered in the sense that the interface tensions Σ_z and Σ_y are nonzero. A change
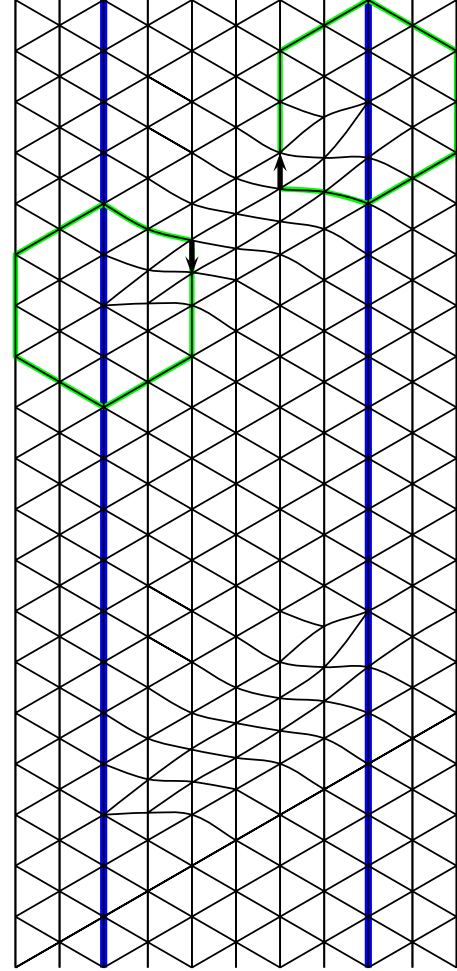

FIG. 6. (Color online) Array of edge dislocations that is located at the defects (thick blue lines) in order to relax shear strain. The Burgers vector is parallel to the defects.

in the boundary conditions with $u_x(x, y, z \to \infty) = u_x(x, y, z \to 0) + \ell$ increases again the energy. Hence the transverse Meissner effect as well as the resistance against FLL shearing perpendicular to the defects is still present. Bond-orientational order[65] persists since disclination pairs remain bounded in the cores of the edge dislocations.

Since the Burgers vectors of the dislocations are always parallel to the defect planes, creep along the x direction is not facilitated. Under the assumption that the distribution of Σ_x is uniform even in the presence of dislocations we recover the creep law of Eq. (95). To describe creep parallel to the defects one has to take into account the interaction between dislocation, a problem not considered so far.[66,67] We leave this for further studies. For weak pinning qualitatively the same behavior can be expected on scales $L_x \gg L_D$, in particular if the defect potential flows under the RG to strong coupling. If the sample exhibits two orthogonal families of (nonintersecting) defects, long-range order in the x and y direction is destroyed even without point impurities on scales larger than L_D. The creep is then limited by the slowest mechanism and hence Eq. (95) is likely to be valid for all current directions in the xy plane.

ACKNOWLEDGMENTS

APPENDIX A: REPLICA HAMILTONIAN FOR THE DEFECT FREE SYSTEM

In this appendix the Hamiltonian for defect-free system is derived, using the replica approach for averaging over point impurities. The pinning energy of randomly distributed impurities reads (see Sec. II)

$$\mathcal{H}_P = \int d^3\mathbf{r} \, V_P(\mathbf{r})\rho_0\left\{-\nabla_{\mathbf{x}}\mathbf{u}(\mathbf{r}) + \sum_{\mathbf{G}\neq 0} e^{i\mathbf{G}[\mathbf{x}-\mathbf{u}(\mathbf{r})]}\right\}, \quad (A1)$$

where $\mathbf{x}=(x,y)$. If the system is characterized by a roughness exponent ζ, displacements vary with the scale L as $u\sim L^\zeta$, $\zeta<1$. The elastic energy scales as $L^{d-2+2\zeta}$, and the first and second terms of Eq. (A1) scale as $L^{(d-2+2\zeta)/2}$ and $L^{d/2}$, respectively. These simple scaling arguments show that the coupling of the divergence of the displacement field to the disorder potential is irrelevant with respect to the elastic energy in $d>2$ and the second term of Eq. (A1) is relevant for $d<4$. Since we are interested in the behavior on large length scales in $d=3$ dimensions, we can neglect the first term of Eq. (A1). After performing the disorder average, the replicated pinning energy reads

$$\mathcal{H}_P^n \approx -\frac{v_p^2 n_{imp}\rho_0^2}{2T}\sum_{\alpha,\beta=1}^n \int_{\mathbf{r},\mathbf{r}'}\delta_\xi(\mathbf{x}-\mathbf{x}')\delta(z-z')$$

$$\times \sum_{\mathbf{G},\mathbf{G}'\neq 0} e^{i\mathbf{G}[\mathbf{x}-\mathbf{u}^\alpha(\mathbf{r})]+i\mathbf{G}'[\mathbf{x}'-\mathbf{u}^\beta(\mathbf{r}')]}$$

$$= -\frac{v_p^2 n_{imp}\rho_0^2}{2T}\sum_{\alpha,\beta=1}^n \int_{z,\mathbf{x}}\sum_{\mathbf{G}\neq 0} e^{i\mathbf{G}[\mathbf{x}-\mathbf{u}^\alpha(\mathbf{x},z)]}$$

$$\times \sum_{\mathbf{G}'\neq 0}\int_{\mathbf{x}_r}\delta_\xi(\mathbf{x}_r)e^{i\mathbf{G}'[\mathbf{x}+\mathbf{x}_r-\mathbf{u}^\beta(\mathbf{x}+\mathbf{x}_r,z)]}$$

$$\approx -\frac{v_p^2 n_{imp}\rho_0^2}{2T}\sum_{\alpha,\beta=1}^n \int_{z,\mathbf{x}}\sum_{\mathbf{G},\mathbf{G}'\neq 0} e^{i\mathbf{x}(\mathbf{G}+\mathbf{G}')}$$

$$\times e^{-i[\mathbf{G}\mathbf{u}^\alpha(\mathbf{x},z)+\mathbf{G}'\mathbf{u}^\beta(\mathbf{x},z)]}\delta_{\xi^{-1}}(\mathbf{G}'). \quad (A2)$$

Using the relative coordinate $\mathbf{x}_r=\mathbf{x}'-\mathbf{x}$ and the fact that $\delta_\xi(\mathbf{x}_r)$ is nonzero only for $|\mathbf{x}_r|\leq\xi$, we approximate the slowly varying displacement field as $\mathbf{u}^\beta(\mathbf{x}+\mathbf{x}_r,z)\approx\mathbf{u}^\beta(\mathbf{x},z)$, where $\delta_{\xi^{-1}}(\mathbf{G})$ is the Fourier transform of $\delta_\xi(\mathbf{x})$. Since the displacement field varies slowly on the scale of the FLL constant, the integral over $\mathbf{x}$ vanishes for all combinations of $\mathbf{G}$ and $\mathbf{G}'$ except for $\mathbf{G}=-\mathbf{G}'$ when the oscillatory factor $e^{i\mathbf{x}(\mathbf{G}+\mathbf{G}')}$ becomes one. The replicated pinning Hamiltonian can now be written as

$$\mathcal{H}_P^n = -\frac{v_p^2 n_{imp}\rho_0^2}{2T}\sum_{\alpha,\beta=1}^n \int_{\mathbf{r}}\sum_{\mathbf{G}\neq 0} e^{i\mathbf{G}[\mathbf{u}^\alpha(\mathbf{r})-\mathbf{u}^\beta(\mathbf{r})]}\delta_{\xi^{-1}}(\mathbf{G})$$

$$= -\frac{1}{2T}\sum_{\alpha,\beta=1}^n \int_{\mathbf{r}} R_P[\mathbf{u}^\alpha(\mathbf{r}) - \mathbf{u}^\beta(\mathbf{r})]. \quad (A3)$$

APPENDIX B: EFFECTIVE HAMILTONIAN ON THE DEFECT PLANE

In this appendix we present a functional-integral approach for the derivation of the effective Hamiltonian on the defect plane for the case of a FLL with point impurities and a single defect plane. Since the pinning energy of the planar defect involves only the displacement perpendicular to the defect, u_x, we integrate out u_x outside the defect and u_y across the entire sample. The partition function can be written as

$$Z = \int \mathcal{D}\varphi(\mathbf{r}_D) \int \mathcal{D}\mathbf{u}(\mathbf{r}) e^{-\mathcal{H}/T}\prod_{\mathbf{r}_D}\delta[u_x(\mathbf{r}_D) - \varphi(\mathbf{r}_D)], \quad (B1)$$

where $\mathcal{H}=\mathcal{H}_0+\mathcal{H}_P+\mathcal{H}_D$. The displacement at the defect is constrained to be $u_x(\mathbf{r}_D)=\varphi(\mathbf{r}_D)$ and this constraint is implemented by δ functions in the functional integral. The defect is aligned to the magnetic field and $\mathbf{r}_D$ is given by Eq. (20). After averaging over point impurities we get

$$\overline{Z^n} = \int \mathcal{D}[\varphi^\alpha(\mathbf{r}_D)]e^{-\Sigma_\alpha\mathcal{H}_D(\varphi^\alpha)/T}\int \mathcal{D}[\mathbf{u}^\alpha(\mathbf{r})]e^{-\mathcal{H}_0^n/T}$$

$$\times \prod_{\alpha,\mathbf{r}_D}\delta[u_x^\alpha(\mathbf{r}_D) - \varphi^\alpha(\mathbf{r}_D)]$$

$$= \int \mathcal{D}[\varphi^\alpha(\mathbf{r}_D)]e^{-\mathcal{H}_{eff}^n(\varphi^\alpha)/T}, \quad (B2)$$

where $\mathcal{H}_0^n$ is given by Eq. (16) and $\int\mathcal{D}[\varphi^\alpha(\mathbf{r}_D)]=\Pi_{\alpha=1}^n\int\mathcal{D}\varphi^\alpha(\mathbf{r}_D)$. Using the function integral representation

$$\prod_{\alpha,\mathbf{r}_D}\delta[u_x^\alpha(\mathbf{r}_D) - \varphi^\alpha(\mathbf{r}_D)]$$

$$= \int \mathcal{D}[\Lambda^\alpha(\mathbf{r}_D)]e^{i\Sigma_\alpha\int_{\mathbf{r}_D}\Lambda^\alpha(\mathbf{r}_D)[u_x^\alpha(\mathbf{r}_D)-\varphi^\alpha(\mathbf{r}_D)]} \quad (B3)$$

of the δ function, we obtain for the effective replica Hamiltonian $\mathcal{H}_{eff}^n$ the equation

$$e^{-\mathcal{H}_{eff}^n/T} = e^{-\Sigma_\alpha\mathcal{H}_D(\varphi^\alpha)/T}\int \mathcal{D}[\Lambda^\alpha(\mathbf{r}_D)]$$

$$\times \left\langle e^{i\Sigma_\alpha\int_{\mathbf{r}_D}\Lambda^\alpha(\mathbf{r}_D)[u_x^\alpha(\mathbf{r}_D)-\varphi^\alpha(\mathbf{r}_D)]}\right\rangle_{\mathcal{H}_0^n} \quad (B4)$$

up to a constant. Here $\langle\ldots\rangle_\mathcal{H}$ denotes the thermal average with respect to $\mathcal{H}$. For this average we obtain

$$\left\langle e^{i\Sigma_\alpha\int_{\mathbf{r}_D}\Lambda^\alpha(\mathbf{r}_D)[u_x^\alpha(\mathbf{r}_D)-\varphi^\alpha(\mathbf{r}_D)]}\right\rangle_{\mathcal{H}_0^n}$$

$$= e^{-i\Sigma_\alpha\int_{\mathbf{r}_D}\Lambda^\alpha(\mathbf{r}_D)\varphi^\alpha(\mathbf{r}_D)}$$

$$\times e^{-\Sigma_{\alpha,\beta}1/2\int_{\mathbf{r}_{D1},\mathbf{r}_{D2}}\Lambda^\alpha(\mathbf{r}_{D1})\Lambda^\beta(\mathbf{r}_{D2})T\mathcal{G}_{xx}^{\alpha,\beta}(\mathbf{r}_{D1}-\mathbf{r}_{D2})}, \quad (B5)$$

where $\langle \tilde{u}_x^\alpha(\mathbf{q}) \tilde{u}_x^\beta(\mathbf{q}')\rangle_{\mathcal{H}_0^n} = T(2\pi)^d \tilde{\mathcal{G}}_{xx}^{\alpha,\beta}(\mathbf{q})\delta(\mathbf{q}+\mathbf{q}')$. The effective Hamiltonian reads

$$
\mathcal{H}_{eff}^n = -\sum_\alpha \sum_{k>0} 2v_k \rho_0 \int d\mathbf{r}_D \cos\{kG_D[\delta - \varphi^\alpha(\mathbf{r}_D)]\}
$$
$$
+ \frac{1}{2}\sum_{\alpha,\beta}\frac{1}{(2\pi)^{d-1}}\int d^{d-1}\mathbf{q}\,\varphi^\alpha(\mathbf{q})\tilde{\mathcal{Q}}_{\alpha,\beta}^{-1}(\mathbf{q})\varphi^\beta(-\mathbf{q}),
$$
(B6)

where $\tilde{\mathcal{Q}}(\mathbf{q})=\tilde{\mathcal{G}}_{xx}(x=0,\mathbf{q})$ and here $\mathbf{q}$ is the in-plane momentum.

APPENDIX C: DENSITY OSCILLATIONS IN THE PRESENCE OF AN IRRELEVANT DEFECT PLANE

In this appendix we analyze the thermal and disorder average of the FL density around an irrelevant defect plane in the presence of point impurities by perturbation theory in v. For the local density variations we have

$$
\overline{\langle \delta\rho[\mathbf{r},\mathbf{u}(\mathbf{r})]\rangle}
$$
$$
= \lim_{n\to 0}\int \mathcal{D}[\mathbf{u}^\alpha]\delta\rho[\mathbf{r},\mathbf{u}_1(\mathbf{r})]e^{-\beta[\mathcal{H}_0^n + \Sigma_\alpha \mathcal{H}_D(u_x^\alpha)]}, \quad (C1)
$$

where $\delta\rho[\mathbf{r},\mathbf{u}(\mathbf{r})]=\rho[\mathbf{r},\mathbf{u}(\mathbf{r})]-\rho_0$ and $u_1(\mathbf{r})$ is the displacement field with replica index $\alpha=1$. To the zeroth order we get

$$
\overline{\langle \delta\rho[\mathbf{r},\mathbf{u}(\mathbf{r})]\rangle} = \lim_{n\to 0}\langle \delta\rho[\mathbf{r},\mathbf{u}_1(\mathbf{r})]\rangle_{\mathcal{H}_0^n} = 0, \quad (C2)
$$

since $\langle u^2(\mathbf{r})\rangle_{\mathcal{H}_0^n}=\infty$. To capture the physics correctly, we have to calculate mean FL density at least to first order in v (see the discussion in Sec. III D 1),

$$
\langle \delta\rho[\mathbf{r},\mathbf{u}(\mathbf{r})]\rangle = -\beta\lim_{n\to 0}\sum_{\alpha=1}^n \langle \delta\rho[\mathbf{r},\mathbf{u}_1(\mathbf{r})]\mathcal{H}_D(\mathbf{u}^\alpha)\rangle_{\mathcal{H}_0^n}
$$
$$
= \beta\lim_{n\to 0}\{\langle \delta\rho[\mathbf{r},\mathbf{u}_1(\mathbf{r})]\mathcal{H}_D(\mathbf{u}_2)\rangle_{\mathcal{H}_0^n}
$$
$$
- \langle \delta\rho[\mathbf{r},\mathbf{u}_1(\mathbf{r})]\mathcal{H}_D(\mathbf{u}_1)\rangle_{\mathcal{H}_0^n}\}. \quad (C3)
$$

$u_2(\mathbf{r})$ is the displacement field with replica index $\alpha=2$. First, we obtain the average of the long wavelength part of the FL density. It can be shown that

$$
\langle \nabla_{\mathbf{x}}\mathbf{u}^\beta(\mathbf{r})\cos[G_D\delta - \mathbf{G}_D\mathbf{u}^\alpha(\mathbf{r}_D)]\rangle_{\mathcal{H}_0^n}
$$
$$
= \nabla_{\mathbf{x}}\{T\sin(G_D\delta)\langle\cos[\mathbf{G}_D\mathbf{u}^\alpha(\mathbf{r}_D)]\rangle_{\mathcal{H}_0^n}\mathcal{G}^{\alpha,\beta}(\mathbf{r}_D-\mathbf{r})|\mathbf{G}_D\rangle
$$
$$
- T\cos(G_D\delta)\langle\sin[\mathbf{G}_D\mathbf{u}^\alpha(\mathbf{r}_D)]\rangle_{\mathcal{H}_0^n}\mathcal{G}^{\alpha,\beta}(\mathbf{r}_D-\mathbf{r})|\mathbf{G}_D\rangle\}, \quad (C4)
$$

where $\mathbf{r}=(\mathbf{x},z)$ and $\mathcal{G}^{\alpha,\beta}(\mathbf{r})$ is the propagator given by Eq. (17). Since $\langle\sin[\mathbf{G}_D\mathbf{u}^\alpha(\mathbf{r}_D)]\rangle_{\mathcal{H}_0^n}=\langle\cos[\mathbf{G}_D\mathbf{u}^\alpha(\mathbf{r}_D)]\rangle_{\mathcal{H}_0^n}=0$ this contribution vanishes.

A finite difference between the expressions $\langle\delta\rho(\mathbf{u}_1)\mathcal{H}_D(\mathbf{u}_2)\rangle_{\mathcal{H}_0^n}$ and $\langle\delta\rho(\mathbf{u}_1)\mathcal{H}_D(\mathbf{u}_1)\rangle_{\mathcal{H}_0^n}$ appearing in Eq. (C3) can result from the thermal part of the propagator that is diagonal in replica indices,

$$
\lim_{n\to 0}\langle \delta\rho[\mathbf{u}^\alpha(\mathbf{r})]\mathcal{H}_D(\mathbf{u}^\beta)\rangle_{\mathcal{H}_0^n}
$$
$$
= \lim_{n\to 0}\left\{\frac{2v_1\rho_0^2}{T}\int_{\mathbf{r}_D}\sum_{\mathbf{G}\neq 0} e^{i\mathbf{G}\cdot\mathbf{x}}\langle e^{-i\mathbf{G}\cdot\mathbf{u}^\alpha(\mathbf{r})}\right.
$$
$$
\times \cos\{G_D[\delta - u_x^\beta(\mathbf{r}_D)]\}\rangle_{\mathcal{H}_0^n}\bigg\}
$$
$$
= \lim_{n\to 0}\left\{\frac{v_1\rho_0^2}{T}\int_{\mathbf{r}_D}\sum_{\mathbf{G}\neq 0} e^{i\mathbf{G}\cdot\mathbf{x}}(e^{iG_D\delta}I_+ + e^{-iG_D\delta}I_-)\right\},
$$
(C5)

where $I_\pm = e^{-1/2\langle[\mathbf{G}\cdot\mathbf{u}^\alpha(\mathbf{r})\pm G_D\cdot\mathbf{u}^\beta(\mathbf{r}_D)]^2\rangle_{\mathcal{H}_0^n}}$ and $\int_{\mathbf{r}_D}$ denotes the integration along the defect plane. Analyzing I_+ (I_-), we conclude that it is nonzero only for $\mathbf{G}=-\mathbf{G}_D$ ($\mathbf{G}=\mathbf{G}_D$) and

$$
I_\pm \approx e^{G_D^2 T\delta_{\alpha,\beta}/(4\pi c|\mathbf{r}-\mathbf{r}_D|)}\left(\frac{L_a}{|\mathbf{r}-\mathbf{r}_D|}\right)^{2g}. \quad (C6)
$$

This yields

$$
\overline{\langle \delta\rho(\mathbf{r})\rangle} \approx \frac{v_1\rho_0^2}{T}(e^{-iG_D(x-\delta)}
$$
$$
+ e^{iG_D(x-\delta)}\int_{\mathbf{r}_D}\left(\frac{L_a}{|\mathbf{r}-\mathbf{r}_D|}\right)^{2g}(e^{G_D^2 T/(4\pi c|\mathbf{r}-\mathbf{r}_D|)}-1)
$$
$$
\approx \frac{4\pi v_1\rho_0^2 L_a^2}{T}\cos[G_D(x-\delta)]
$$
$$
\times \left(\frac{G_D^2 T}{2\pi c}\right)^{2-2g}F\left(\frac{G_D^2 T}{4\pi c|x-\delta|}\right), \quad (C7)
$$

where $F(x)=\sum_{n=1}^\infty \frac{1}{n!}\frac{x^{2g+n-2}}{2g+n-2}$. For very small temperatures the main contribution is

$$
\overline{\langle \delta\rho(\mathbf{r})\rangle} \approx \frac{v_1\rho_0^2 G_D^2 L_a}{c(2g-1)}\cos[G_D(x-\delta)]\left(\frac{L_a}{|x-\delta|}\right)^{2g-1} + \mathcal{O}(T). \quad (C8)
$$

The result captures the large scale behavior since it is valid on scales larger than $L\geq L_a$. Here v_1 denotes the effective defect strength measured on the scale L_a, and $|x-\delta|$ is the distance to the defect plane. Additional contributions to Eq. (C8), coming from the higher harmonics in $\mathcal{H}_D$, are less important since they are proportional to the coefficients v_k at scale $L=L_a$ and their amplitudes decay as $|x-\delta|^{-2k^2 g+1}$ with integer $k\geq 2$.

APPENDIX D: DENSITY OSCILLATIONS IN THE PRESENCE OF A RELEVANT DEFECT PLANE

In this appendix we study the displacement correlation functions and average FL density profile for a relevant defect plane in the presence of point impurities. As shown in the main text above, on sufficiently large length scales pinning effects can be taken into account through the boundary condition $u_x(\mathbf{r}_D)=0$ at the defect plane. For simplicity we take the defect to be at the coordinate origin, i.e., we set $\delta=0$. First we calculate the generating function

$$\overline{Z^n[\mathbf{j}^\alpha(\mathbf{r})]} = \int \mathcal{D}[\mathbf{u}^\alpha] e^{-\mathcal{H}_0^n[\mathbf{u}^\alpha]/T} e^{\Sigma_\alpha \int_\mathbf{r} \mathbf{j}^\alpha(\mathbf{r})\mathbf{u}^\alpha(\mathbf{r})} \prod_{\alpha,\mathbf{r}_D} \delta[u_x^\alpha(\mathbf{r}_D)].$$
(D1)

Using the representation of the delta function of Eq. (B3) we get

$$\overline{Z^n[\mathbf{j}^\alpha(\mathbf{r})]} = e^{T/2\Sigma_{\alpha,\beta}\int_{\mathbf{r}_1,\mathbf{r}_2} \mathbf{j}^\alpha(\mathbf{r}_1)\Gamma^{\alpha,\beta}(\mathbf{r}_1,\mathbf{r}_2)\mathbf{j}^\beta(\mathbf{r}_2)}, \quad (D2)$$

where

$$\Gamma^{\alpha\beta}(\mathbf{r}_1,\mathbf{r}_2) = \mathcal{G}^{\alpha\beta}(\mathbf{r}_1 - \mathbf{r}_2) - \sum_{\gamma\kappa} \int_{\mathbf{r}_{D1}\mathbf{r}_{D2}} \mathcal{G}^{\alpha\gamma}(\mathbf{r}_1 - \mathbf{r}_{D1})$$

$$\times |\hat{\mathbf{x}}\rangle \widetilde{\mathcal{Q}}_{\gamma\kappa}^{-1}(\mathbf{r}_{D1} - \mathbf{r}_{D2})\langle\hat{\mathbf{x}}|\mathcal{G}^{\kappa\beta}(\mathbf{r}_2 - \mathbf{r}_{D2}) \quad (D3)$$

and $\widetilde{\mathcal{Q}}$ is given by Eq. (31) and $\mathcal{G}^{\alpha,\beta}$ is the inverse of $\mathcal{G}_{\alpha,\beta}^{-1}$ given by Eq. (17). The displacement correlation function is given by the relation $\overline{\langle\mathbf{u}(\mathbf{r})\mathbf{u}(\mathbf{r})\rangle} = \lim_{n\to 0} \frac{\delta^2 Z^n}{\delta\mathbf{j}^1(\mathbf{r})\delta\mathbf{j}^1(\mathbf{r})}|_{j^\alpha=0}$. Denoting by $\mathbf{q}$ the in-plane momentum, we get in momentum space

$$\widetilde{\mathcal{G}}_{pin,ij}(x,x;\mathbf{q}) = \lim_{n\to 0}\bigg[\widetilde{\mathcal{G}}_{ij}^{11}(0,\mathbf{q}) - \sum_{\alpha\gamma} \widetilde{\mathcal{G}}_{ix}^{1\alpha}(|x|,\mathbf{q})\widetilde{\mathcal{Q}}_{\alpha\gamma}^{-1}(\mathbf{q})$$

$$\times \widetilde{\mathcal{G}}_{xj}^{1\gamma}(|x|,-\mathbf{q}) \bigg], \quad (D4)$$

where $\mathcal{G}_{pin,ij}(x,x';\mathbf{r}_\| - \mathbf{r}_\|') = T^{-1}\overline{\langle u_i(\mathbf{r})u_j(\mathbf{r}')\rangle}$ with $\mathbf{r} = (x,\mathbf{r}_\|)$. The indices i,j take the values x,y. All propagators and their inverse that appear in the previous equations have the form $\mathbf{X}_{\alpha,\beta} = \delta_{\alpha,\beta}\mathbf{X}_d + \mathbf{X}_n$, where α,β are replica indices. The only nonzero contribution to the second term of Eq. (D4) comes from the product of all "diagonal" parts ($\mathbf{X}_d$) of the propagators or only one "nondiagonal" ($\mathbf{X}_n$) and two diagonal (in replica indices) in the limit $n\to 0$. Denoting by $X_{ij,a} = \lim_{n\to 0}\langle\hat{i}|\mathbf{X}_a|\hat{j}\rangle$, where $a = d,n$, one has

$$\widetilde{\mathcal{G}}_{pin,ij}(x,x;\mathbf{q}) = \widetilde{\mathcal{G}}_{ij,d}(0,\mathbf{q}) - \widetilde{\mathcal{G}}_{ix,d}(|x|,\mathbf{q})\widetilde{\mathcal{G}}_{jx,d}(|x|,\mathbf{q})\widetilde{\mathcal{Q}}_d^{-1}(\mathbf{q})$$

$$+ \widetilde{\mathcal{G}}_{ij,n}(0,\mathbf{q}) - \widetilde{\mathcal{G}}_{ix,d}(|x|,\mathbf{q})\widetilde{\mathcal{G}}_{jx,d}(|x|,\mathbf{q})\widetilde{\mathcal{Q}}_n^{-1}(\mathbf{q})$$

$$+ \widetilde{\mathcal{Q}}_d^{-1}(\mathbf{q})\widetilde{\mathcal{G}}_{jx,n}(|x|,\mathbf{q})\widetilde{\mathcal{G}}_{ix,d}(|x|,\mathbf{q})$$

$$+ \widetilde{\mathcal{Q}}_d^{-1}(\mathbf{q})\widetilde{\mathcal{G}}_{ix,n}(|x|,\mathbf{q})\widetilde{\mathcal{G}}_{jx,d}(|x|,\mathbf{q}). \quad (D5)$$

For isotropic elasticity the relation

$$\widetilde{\mathcal{G}}_{ix,d}(|x|,\mathbf{q})\widetilde{\mathcal{G}}_{jx,d}(|x|,\mathbf{q})\widetilde{\mathcal{Q}}_d^{-1}(\mathbf{q}) = (\hat{\mathbf{x}}\cdot\hat{\mathbf{i}})(\hat{\mathbf{x}}\cdot\hat{\mathbf{j}})\widetilde{\mathcal{G}}_{ij,d}(2|x|,\mathbf{q})$$
(D6)

holds. After integrating the terms of the second and the third line of Eq. (D5) over $\mathbf{q}$ we find that the displacement correlations on scales larger than L_v [see Eq. (38)] read

$$\overline{\langle u_i(\mathbf{r})u_j(\mathbf{r})\rangle} = \lim_{n\to 0}\{T\mathcal{G}_{ij}^{11}(0,0) - T(\hat{\mathbf{x}}\cdot\hat{\mathbf{i}})(\hat{\mathbf{x}}\cdot\hat{\mathbf{j}})\mathcal{G}_{xx}^{11}(2|x|,0)\}.$$
(D7)

Next, we shall calculate the disorder and thermal average of the FL density

$$\overline{\langle\delta\rho(\mathbf{r})\rangle} = \rho_0 \sum_{\mathbf{G}\neq 0} e^{i\mathbf{G}\mathbf{x}}\overline{\langle e^{-i\mathbf{G}\mathbf{u}}\rangle}, \quad (D8)$$

using

$$\overline{\langle e^{-i\mathbf{G}\mathbf{u}}\rangle} = \lim_{n\to 0}\langle e^{-i\mathbf{G}\mathbf{u}_1}\rangle = \lim_{n\to 0} e^{-1/2\langle(\mathbf{G}\mathbf{u}_1(\mathbf{r}))^2\rangle} \quad (D9)$$

and

$$\lim_{n\to 0}\langle[\mathbf{G}\mathbf{u}_1(\mathbf{r})]^2\rangle = \lim_{n\to 0} T[G^2\mathcal{G}_{xx}^{11}(0) - (\mathbf{G}\cdot\hat{\mathbf{x}})^2\mathcal{G}_{xx}^{11}(2|x|,0)].$$
(D10)

Since $\lim_{n\to 0}\mathcal{G}_{xx}^{11}(0)$ is divergent we conclude that only terms with a reciprocal vector $\mathbf{G}$ perpendicular to the defect plane contribute in Eq. (D8) and

$$\overline{\langle\delta\rho(\mathbf{r})\rangle} = 2\rho_0 \sum_{m>0} \cos(mG_D x)\left(\frac{L_v}{|x|}\right)^{m^2 g}, \quad (D11)$$

where m is an integer number.

APPENDIX E: SAMPLE-TO-SAMPLE FLUCTUATIONS OF THE MAGNETIC SUSCEPTIBILITY

In this appendix we examine the influence of planar defects on the longitudinal magnetic susceptibility. An infinitesimal change in the longitudinal magnetic field $\delta H_z\hat{\mathbf{z}}$ changes the Hamiltonian of Eq. (42) in the case of an uniaxial displacement field perpendicular to the defects by

$$\delta\mathcal{H} = -\frac{\phi_0\rho_0}{4\pi} \int d^3 r \,\delta H_z\partial_x u. \quad (E1)$$

Since the change of the magnetic induction is $B = \rho_0\phi_0\partial_x u$, the longitudinal magnetic susceptibility reads

$$\chi = \rho_0\phi_0\frac{\partial\langle\partial_x u\rangle}{\partial\delta H_z} = -\frac{4\pi}{V}\frac{\partial^2 F}{\partial\delta H_z^2}, \quad (E2)$$

where F is the free energy. It is convenient to consider a generalization of this model to d dimensions where $\mathbf{x}$ is a $d-2$-dimensional vector and x_1 is the component of $\mathbf{x}$ in the direction of the displacement u. Applying the transformation $u \to u + hx_1/c_{11}$, the additional term given by Eq. (E1) can be shifted away yielding

$$\mathcal{H}(h,u) = \mathcal{H}_0(u) - \frac{h^2}{2c_{11}}V + \mathcal{H}_D(u + hx_1/c_{11}), \quad (E3)$$

where $V = L_x^{d-2}L_z L_y$ and $h = \delta H_z\rho_0\phi_0/(4\pi)$. The pinning energy of planar defects $\mathcal{H}_D$ can be written as

$$\mathcal{H}_D(u) = \int d\mathbf{r}\, V_D(\mathbf{x})\rho_s(u,\mathbf{r}) + \int d\mathbf{r}\, V_D(\mathbf{x})\rho_p(u,\mathbf{r}) = \mathcal{H}_D^s + \mathcal{H}_D^p,$$
(E4)

where ρ_s and ρ_p are the slowly varying and periodic part of the FL density, respectively. Next, we would like to compute the average $\bar{\chi}$. The free energy is given by

$$F(h) = -T \log\left(\int \mathcal{D}u e^{-\mathcal{H}(h,u)/T} \right)$$

$$= -\frac{h^2}{2c_{11}}V - \rho_0 \frac{h}{c_{11}} \int d\mathbf{r} V_D(\mathbf{x}) - T \log Z_1, \quad \text{(E5)}$$

where Z_1 is the partition function for $\mathcal{H}_1(h,u) = \mathcal{H}_0(u) + \mathcal{H}_D^s(u) + \mathcal{H}_D^p(u + hx_1/c_{11})$. Using replicas, the disorder averaged free energy can be written as

$$\overline{F} = -\frac{h^2}{2c_{11}}V - T \lim_{n \to 0} \frac{\overline{Z_1^n} - 1}{n}. \quad \text{(E6)}$$

Here $\overline{Z_1^n} = \int \mathcal{D}[u^\alpha] \exp[-\mathcal{H}_1^n/T]$, where $\mathcal{H}_1^n$ is the replica Hamiltonian that follows from $\mathcal{H}_1(h,u)$. Since $\mathcal{H}_1(h,u)$ has the same statistical properties as $\mathcal{H}(0,u)$, i.e., it yields the same replica Hamiltonian, the only dependence on h in $\overline{F}$ comes from the first quadratic term in Eq. (E6). Due to this so-called statistical tilt symmetry,[46] the disorder averaged susceptibility

$$\overline{\chi} = -\frac{4\pi}{V} \frac{\partial^2 \overline{F}}{\partial \delta H_z^2} = \frac{(\rho_0 \phi_0)^2}{4\pi c_{11}} \quad \text{(E7)}$$

is disorder independent. The important quantity is the sample-to-sample variations of the susceptibility. The free energy can be written as

$$F(h) = -\frac{h^2}{2c_{11}}V + F_0 - T \log\langle e^{-\mathcal{H}_D(u + hx_1/c_{11})/T} \rangle_{\mathcal{H}_0}, \quad \text{(E8)}$$

where F_0 is the free energy of the system that is described by the elastic Hamiltonian only. To first order in perturbation theory with respect to $\sim v$ we get

$$\Delta F(h) = F(h) - \overline{F(h)} = \langle \mathcal{H}_D(u + hx_1/c_{11}) \rangle_{\mathcal{H}_0}. \quad \text{(E9)}$$

For a system of linear size L_x in the x direction we find

$$\overline{\Delta F(h_1)\Delta F(h_2)} = 2(v\rho_0)^2 n_{pd}(L_y L_z)^2$$
$$\times \int d\mathbf{x} \sum_{n>0}^{[\ell/\xi]_G} e^{-(nG_D)^2\langle u^2 \rangle_{\mathcal{H}_0}}$$
$$\times \cos\left[nG_D \frac{(h_1 - h_2)x_1}{c_{11}} \right], \quad \text{(E10)}$$

where n_{pd} denotes the density of defects. Differentiation with respect to h_1 and h_2 leads to

$$\frac{\overline{\Delta \chi^2}}{\overline{\chi}^2} = \frac{R_D''''(0)L_x^\epsilon}{5c_{11}^2} \sim \left(\frac{L_x}{L_D} \right)^\epsilon, \quad \text{(E11)}$$

where we have taken into account the irrelevance of thermal fluctuation. Since $\epsilon > 0$ for $d < 6$, the sample-to-sample fluctuations grow with the scale L_x. One cannot expect that this result is quantitatively correct for large L_x. However, qualitatively it demonstrates the relevance of defects and it is a signature of a glassy phase. For $L_x > L_D$ we expect that $\overline{(\Delta \chi)^2}/\overline{\chi}^2$ approaches a finite universal value for $d < 6$.

APPENDIX F: POSITIONAL CORRELATION FUNCTION FOR $6 > d > 4$

In this appendix the positional correlation function of the FLL with planar defects will be calculated, using perturbation theory and results from the functional RG analysis presented in Sec. IV. The positional correlation functions have been calculated before for the FLL with point impurities for an uniaxial displacement field[6,7] and for a vector displacement field.[8,9] We perform the computations along the lines of these references.

In a functional RG procedure, after integrating out fast modes in an infinitesimal shell with $\Lambda/b \leq q \leq \Lambda$, one can choose to keep the cutoff in momentum space fixed using the rescaling

$$\mathbf{x}' = \frac{\mathbf{x}}{b} \quad \mathbf{z}' = \frac{\mathbf{z}}{b^\chi},$$

$$\mathbf{q}_x' = b\mathbf{q}_x \quad \mathbf{q}_z' = b^\chi \mathbf{q}_z, \quad \text{(F1)}$$

where $\mathbf{z} = (y, z)$. The displacement field is not rescaled due to the periodicity of R_D. This implies $u(\mathbf{q}) = b^{d-2+2\chi} u'(\mathbf{q}')$. We need to obtain the RG flow of the correlation function

$$\langle u(\mathbf{q}_1)u(\mathbf{q}_2) \rangle = Z^{-1} \int \mathcal{D}u(\mathbf{q}) e^{-\beta\mathcal{H}} u(\mathbf{q}_1)u(\mathbf{q}_2)$$
$$= Z^{-1} \int \mathcal{D}u^<(\mathbf{q}) u(\mathbf{q}_1)u(\mathbf{q}_2) \int \mathcal{D}u^>(\mathbf{q}) e^{-\beta\mathcal{H}}$$
$$= Z^{-1} \int \mathcal{D}u^<(\mathbf{q}) u(\mathbf{q}_1)u(\mathbf{q}_2) e^{-\beta\mathcal{H}_l(u^<(\mathbf{q}))}$$
$$= b^{2(d-2+2\chi)}\langle u'(\mathbf{q}_1')u'(\mathbf{q}_2') \rangle, \quad \text{(F2)}$$

where $\mathcal{H} = \mathcal{H}_0 + \int V_D(x)\rho(u, \mathbf{r})$. Here $u^<(\mathbf{q})$ are modes that satisfy $q < \Lambda/b$, and $\mathcal{H}_l$ is the Hamiltonian that applies to the scale $l = \log b$ with b very close to unity. Using Eq. (F2), we obtain a differential equation for $\langle u(\mathbf{q}_1)u(\mathbf{q}_2) \rangle$. We get

$$\langle u(\mathbf{q}_1)u(\mathbf{q}_2) \rangle = b^{2(d-2+2\chi)}\langle u'(\mathbf{q}_1')u'(\mathbf{q}_2') \rangle, \quad \text{(F3)}$$

where the only restriction on b is $q_i < \Lambda/b$, $i = 1, 2$.

First, we calculate $\langle u(\mathbf{q}_1)u(\mathbf{q}_2)\rangle$ to lowest order in v,

$$\langle u(\mathbf{q}_1)u(\mathbf{q}_2)\rangle = \langle u(\mathbf{q}_1)u(\mathbf{q}_2)\rangle_{\mathcal{H}_0} + \frac{1}{2T^2}\lim_{n\to 0}$$

$$\times \sum_{\beta,\gamma}\int_{\mathbf{x},\mathbf{z}_1,\mathbf{z}_2}\langle u_1(\mathbf{q}_1)u_1(\mathbf{q}_2)R_D[u^\beta(\mathbf{x},\mathbf{z}_1)$$

$$- u^\gamma(\mathbf{x},\mathbf{z}_2)]\rangle_{\Sigma_\alpha\mathcal{H}_0(u^\alpha)}, \tag{F4}$$

where u_1 is the displacement field with replica index $\alpha=1$. We use the periodicity of R_D by writing $R_D(u) = \Sigma_n R_n \cos(nG_D u)$. From this we find that *at the planar glass fixed point*

$$\langle u(\mathbf{q}_1)u(\mathbf{q}_2)\rangle = \frac{-(2\pi)^{d+2}}{(c_{11}q_{1x}^2)^2}R_D^{*\prime\prime}(0)\,\delta(\mathbf{q}_{1x}+\mathbf{q}_{2x})\delta(\mathbf{q}_{1z})\delta(\mathbf{q}_{2z}),$$
$$\tag{F5}$$

where the rescaled fixed-point correlator is $R_D^{*\prime\prime}(u) = -\frac{\epsilon c_{11}^2 \Lambda^\epsilon}{6K_d}[(u-\ell/2)^2 - \ell^2/12]$ for $0 \le u < \ell$. Choosing $b = \Lambda/\max\{q_{1x}, q_{2x}\}$ in Eq. (F3) so that it is justified to calcu-

late the correlation function appearing on the right-hand side of Eq. (F3) at the fixed point, and using the result of Eq. (F5), we get

$$\langle u(\mathbf{q}_1)u(\mathbf{q}_2)\rangle = \frac{(2\pi)^{2d}}{36 S_{d-2}}\frac{\Lambda^{2(6-d)}}{q_{1x}^{d-2}}\epsilon\ell^2\,\delta(\mathbf{q}_{1x}+\mathbf{q}_{2x})\delta(\mathbf{q}_{1z})\delta(\mathbf{q}_{2z}). \tag{F6}$$

Note that in Eq. (F6) only displacements with $\mathbf{q}_{1x}=-\mathbf{q}_{2x}$ are coupled as it would be the case for a quadratic Hamiltonian. Therefore one can write down an effective quadratic Hamiltonian in the $\mathbf{q}_x$-momentum space that reproduces the correlations to first order in ϵ. The positional correlation function shows the power low behavior

$$S_{G_D} \approx |\mathbf{x}|^{-\epsilon(\pi/3)^2}. \tag{F7}$$

We point out that this result is valid only for $d > 4$. In $d \le 4$ dimensions the part of the pinning potential related to the slowly varying part of the FL density also becomes relevant and further analysis is needed (see Sec. IV).

APPENDIX G: LIST OF RECURRENT SYMBOLS

Symbol	Quantity	Definition
a	Flux-line lattice constant	
$\mathbf{B}$	Magnetic induction	
c_{ii} $i=1,4,6$	Elastic constants	Eq. (2)
$\mathbf{G}$	Reciprocal-lattice vector	
$g=\frac{3}{8}\eta(\frac{a}{\ell})^2$	Parameter controlling the relevance of the single defect plane	Eq. (25)
$G_D=\frac{2\pi}{\ell}$	Shortest reciprocal-lattice vector perpendicular to the defect(s)	Sec. III
$\mathcal{H}_0$	Elastic energy of distortions of the FLL	Eq. (2)
$\mathcal{H}_P$	Pinning energy of point impurities	Eq. (5)
$\mathcal{H}_0^n$	Effective quadratic replica Hamiltonian for the defect-free Bragg glass	Eq. (16)
$\mathcal{H}_D$	Pinning energy of a planar defect	Eq. (22)
J	Current density	
L_ξ	Larkin length	Eq. (10)
L_a	Positional correlation length	Sec. II
ℓ_D	Mean distance between defects	Sec. IV
L_D	Larkin length for planar defects	Sec. IV
n_{imp}	Density of point impurities	
n_D	Unit vector perpendicular to the defect plane	
$\mathbf{r}_D$	Position vector of the defect plane	Eq. (20)
R_P	Point disorder correlation function	Eq. (14)
R_D	Planar disorder correlation function	Eq. (46)
R_D^*	Fixed-point value of R_D	
$S_{\mathbf{G}}(\mathbf{r})$	Positional correlation function	Sec. II
S_d	Surface of d dimensional unit sphere	
T	Temperature	
$u_i(y,z)=u(x_i,y,z)$	Displacement field at the planar defect with $x=x_i$	
u_x	Displacement field perpendicular to the defects	
v_p	Strength of point impurities	Sec. II
V_P	Pinning potential resulting from point impurities	Eq. (2)

Symbol	Quantity	Definition
v	Planar defect strength	Sec. III
V_D	Pinning potential resulting from planar defects	Sec. IV
$[x]_G$	The closest integer to x	
δ	Defect distance to the origin	
ζ	Roughness coefficient	Sec. II
η	Power-law exponent of positional correlation function in the Bragg glass regime	Sec. II
Λ	Momentum cutoff	Sec. II
λ	Penetration depth	Sec. II
ξ_{RF}	Roughness exponent in random force regime	Sec. II
ξ_{RM}	Roughness exponent in random manifold regime	Sec. II
ξ_{BG}	Roughness exponent in the Bragg glass regime	Sec. II
ξ	Superconductor coherence length	
ξ_c	Correlation length	
$\rho(\mathbf{u},\mathbf{r})$	Flux-line density	Eq. (6)
ρ_0	Background FL density	Eq. (6)
$\Sigma_{y(z)}$	Interface tension of a domain wall perpendicular to z (y) axis	Eq. (51)
ϕ_0	Flux quantum	Sec. II

[1] M. Tinkham, *Introduction to Superconductivity*, 2nd ed. (McGraw-Hill, New York, 1996).

[2] J. Bardeen and M. J. Stephen, Phys. Rev. **140**, A1197 (1965).

[3] G. Blatter, M. V. Feigel'man, V. B. Geshkenbein, A. I. Larkin, and V. M. Vinokur, Rev. Mod. Phys. **66**, 1125 (1994).

[4] T. Nattermann, Phys. Rev. Lett. **64**, 2454 (1990).

[5] A. I. Larkin, Sov. Phys. JETP **31**, 784 (1970).

[6] T. Giamarchi and P. Le Doussal, Phys. Rev. Lett. **72**, 1530 (1994).

[7] T. Giamarchi and P. Le Doussal, Phys. Rev. B **52**, 1242 (1995).

[8] T. Emig, S. Bogner, and T. Nattermann, Phys. Rev. Lett. **83**, 400 (1999).

[9] S. Bogner, T. Emig, and T. Nattermann, Phys. Rev. B **63**, 174501 (2001).

[10] T. Klein, I. Joumard, S. Blanchard, J. Marcus, R. Cubitt, T. Giamarchi, and P. Le Doussal, Nature (London) **413**, 404 (2001).

[11] D. R. Nelson and V. M. Vinokur, Phys. Rev. Lett. **68**, 2398 (1992).

[12] D. R. Nelson and V. M. Vinokur, Phys. Rev. B **48**, 13060 (1993).

[13] I. F. Lyuksyutov, Europhys. Lett. **20**, 273 (1992).

[14] L. Radzihovsky, Phys. Rev. Lett. **74**, 4923 (1995).

[15] T. Roy and T. E. Mitchell, Philos. Mag. A **63**, 225 (1991).

[16] G. W. Crabtree, W. K. Kwok, U. Welp, S. F. J. Downey, K. G. Vandervoort, and J. Z. Liu, Physica C **185-189**, 282 (1991).

[17] W. K. Kwok, S. Fleshler, U. Welp, V. M. Vinokur, J. Downey, G. W. Crabtree, and M. M. Miller, Phys. Rev. Lett. **69**, 3370 (1992).

[18] M. Oussena, P. A. J. de Groot, K. Deligiannis, A. V. Volkozub, R. Gagnon, and L. Taillefer, Phys. Rev. Lett. **76**, 2559 (1996).

[19] S. Sanfilippo, D. Bourgault, C. Villard, R. Tournier, P. G. Picard, E. Beaugnon, A. Sulpice, T. Fournier, and P. Germi, Europhys. Lett. **39**, 657 (1997).

[20] M. C. Marchetti and V. M. Vinokur, Phys. Rev. B **51**, 16276 (1995).

[21] G. J. Dolan, G. V. Chandrashekhar, T. R. Dinger, C. Feild, and F. Holtzberg, Phys. Rev. Lett. **62**, 827 (1989).

[22] L.-H. Tang and I. F. Lyuksyutov, Phys. Rev. Lett. **71**, 2745 (1993).

[23] L. Balents and M. Kardar, Europhys. Lett. **23**, 503 (1993).

[24] L. Balents and M. Kardar, Phys. Rev. B **49**, 13030 (1994).

[25] T. Hwa and T. Nattermann, Phys. Rev. B **51**, 455 (1995).

[26] T. Emig and T. Nattermann, Phys. Rev. Lett. **97**, 177002 (2006).

[27] A. Petković and T. Nattermann, Phys. Rev. Lett. **101**, 267005 (2008).

[28] W. Hofstetter, I. Affleck, D. R. Nelson, and U. Schollwöck, Europhys. Lett. **66**, 178 (2004).

[29] I. Affleck, W. Hofstetter, D. R. Nelson, and U. Schollwöck, J. Stat. Mech.: Theor. Exp. (2004) P10003.

[30] L. Radzihovsky, Phys. Rev. B **73**, 104504 (2006).

[31] C. L. Kane and M. P. A. Fisher, Phys. Rev. B **46**, 15233 (1992).

[32] R. Egger and H. Grabert, Phys. Rev. Lett. **75**, 3505 (1995).

[33] G. Grüner, Rev. Mod. Phys. **60**, 1129 (1988).

[34] A. D. Bruce and R. A. Cowley, J. Phys. C **11**, 3609 (1978).

[35] L. Balents and D. R. Nelson, Phys. Rev. Lett. **73**, 2618 (1994).

[36] L. D. Landau and E. M. Lifshitz, *Elasticity theory*, 2nd ed. (Elsevier, New York, 2004).

[37] M. V. Feigel'man, V. B. Geshkenbein, A. I. Larkin, and V. M. Vinokur, Phys. Rev. Lett. **63**, 2303 (1989).

[38] S. E. Korshunov, Phys. Rev. B **48**, 3969 (1993).

[39] M. Kardar, J. Appl. Phys. **61**, 3601 (1987).

[40] T. Nattermann, Europhys. Lett. **4**, 1241 (1987).

[41] M. Laver, E. M. Forgan, A. B. Abrahamsen, C. Bowell, Th. Geue, and R. Cubitt, Phys. Rev. Lett. **100**, 107001 (2008).

[42] P. Le Doussal and K. J. Wiese, Phys. Rev. E **68**, 046118 (2003).

[43] T. Hwa and D. S. Fisher, Phys. Rev. Lett. **72**, 2466 (1994).

[44] J. Kierfeld and V. M. Vinokur, Phys. Rev. B **61**, R14928 (2000).

[45] Since the defects are weak, the effects we are interested in become visible on large length scales. Hence, we can introduce a coarse-grained version of the defect potential $\widetilde{V}(x)$ $= \int dx' V_D(x')/L_w$, where the integration is over a segment of length $L_w \gg \ell_D$. In that case the central limit theorem shows that $\widetilde{V}(x)$ is Gaussian distributed with $\overline{\widetilde{V}(x)\widetilde{V}(x')} = v^2/\ell_D \delta(x-x')$. In the planar defect Hamiltonian, the slowly varying part of the FL density couples only to $\mu(x) = \int_{|q_x| \sim 0} \widetilde{V}(q_x) \exp[iq_x x]/(2\pi)$, while to the periodic part of the FL density couples $W(x)$ $= \Sigma_n \int_{|q_x| \sim 0} \widetilde{V}(nG_D+q_x) \exp[i(q_x+nG_D)x]/(2\pi)$, where $n \neq 0$ is an integer number. Since the Gaussian distributed potential satisfies $\overline{\widetilde{V}(q)\widetilde{V}(q')} = 2\pi v^2/\ell_D \delta(q+q')$, the potentials $\mu(x)$ and $W(x)$ are not correlated, $\overline{W(x)\mu(x)} = 0$. By applying the transformation $u'(\mathbf{r}) = u(\mathbf{r}) - \int_0^x dx_1 \mu(x_1)/c_{11}$ and averaging over $W(x)$, we get only the second term of the replica Hamiltonian of Eq. (45) and the first term has been eliminated.

[46] U. Schulz, J. Villian, E. Brezin, and H. Orland, J. Stat. Phys. **51**, 1 (1988).

[47] V. G. Kogan and L. J. Campbell, Phys. Rev. Lett. **62**, 1552 (1989).

[48] J. Imry and S. K. Ma, Phys. Rev. Lett. **35**, 1399 (1975).

[49] D. S. Fisher, Phys. Rev. Lett. **56**, 1964 (1986).

[50] L. Balents and D. S. Fisher, Phys. Rev. B **48**, 5949 (1993).

[51] L. Balents, Europhys. Lett. **24**, 489 (1993).

[52] A. A. Fedorenko, Phys. Rev. B **77**, 094203 (2008).

[53] T. Nattermann, S. Stepanow, L. H. Tang, and H. Leschhorn, J. Phys. II France **2**, 1483 (1992).

[54] T. Nattermann and S. Scheidl, Adv. Phys. **49**, 607 (2000).

[55] J. Villain and J. F. Fernandez, Z. Phys. B: Condens. Matter **54**, 139 (1984).

[56] M. V. Feigelman, Sov. Phys. JETP **52**, 3 (1980).

[57] S. V. Malininand T. Nattermann, Int. J. Mod. Phys. B **21**, 4164 (2007).

[58] A. Glatz and T. Nattermann, Phys. Rev. B **69**, 115118 (2004).

[59] J. H. V. Hoff, *Etudes de Dynamiques Chimiques* (F. Muller and Co., Amsterdam, 1884).

[60] S. Arrhenius, Z. Phys. Chem. **4**, 226 (1889).

[61] T. Giamarchi, *Quantum Physics in One Dimension*, 1st ed. (Clarendon, Oxford, 2003), Chap. 10.

[62] S. V. Malinin, T. Nattermann, and B. Rosenow, Phys. Rev. B **70**, 235120 (2004).

[63] E. H. Brandt, Phys. Rev. B **34**, 6514 (1986).

[64] P. F. Arndt and T. Nattermann, Phys. Rev. B **63**, 134204 (2001).

[65] B. I. Halperin and D. R. Nelson, Phys. Rev. Lett. **41**, 121 (1978).

[66] J. Kierfeld, H. Nordborg, and V. M. Vinokur, Phys. Rev. Lett. **85**, 4948 (2000).

[67] P. Moretti, M. Carmen Miguel, M. Zaiser, and S. Zapperi, Phys. Rev. B **69**, 214103 (2004).